# Structure−Activity Relationships and Optimization of 3,5-Dichloropyridine Derivatives As Novel P2X7 Receptor Antagonists

Won-Gil Lee,[†] So-Deok Lee,[†] Joong-Heui Cho,[†] Younghwan Jung,[†] Jeong-hyun Kim,[†] Tran T. Hien,[‡] Keon-Wook Kang,[‡] Hyojin Ko,[§] and Yong-Chul Kim*[,†,§]

[†]School of Life Sciences, Gwangju Institute of Science and Technology (GIST), Gwangju 500-712, Republic of Korea

[‡]College of Pharmacy, Seoul National University, Seoul, Republic of Korea

[§]Graduate Program of Medical System Engineering, Gwangju Institute of Science and Technology (GIST), Gwangju 500-712, Republic of Korea

Ⓢ Supporting Information

**ABSTRACT:** Screening of a library of chemical compounds showed that the dichloropyridine-based analogue **9** was a novel P2X7 receptor antagonist. To optimize its activity, we assessed the structure−activity relationships (SAR) of **9**, focusing on the hydrazide linker, the dichloropyridine skeleton, and the hydrophobic acyl ($R_2$) group. We found that the hydrazide linker and the 3,5-disubstituted chlorides in the pyridine skeleton were critical for P2X7 antagonistic activity and that the presence of hydrophobic polycycloalkyl groups at the $R_2$ position optimized antagonistic activity. In the EtBr uptake assay in $hP2X_7$-expressing HEK293 cells, the optimized antagonists, **51** and **52**, had $IC_{50}$ values of 4.9 and 13 nM, respectively. The antagonistic effects of



EtBr Assay, $IC_{50}$ 650 nM
IL-1$\beta$ ELISA, $IC_{50}$ 320 nM

EtBr Assay, $IC_{50}$ 13 nM
IL-1$\beta$ ELISA, $IC_{50}$ 9.2 nM

**51** and **52** were paralleled by their ability to inhibit the release of the pro-inflammatory cytokine, IL-1$\beta$, by LPS/IFN-$\gamma$/BzATP stimulation of THP-1 cells ($IC_{50}$ = 1.3 and 9.2 nM, respectively). In addition, **52** strongly inhibited iNOS/COX-2 expression and NO production in THP-1 cells, further indicating that this compound blocks inflammatory signaling and suggesting that the dichloropyridine analogues may be useful in developing P2X7 receptor targeted anti-inflammatory agents.
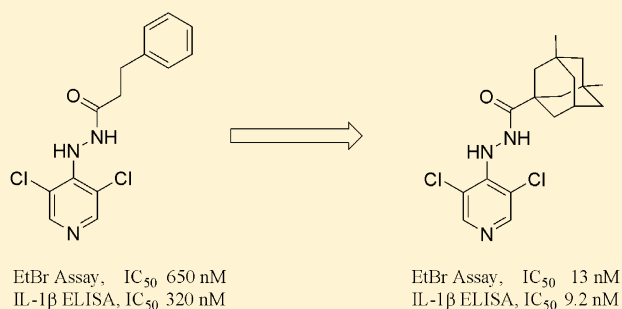
## ■ INTRODUCTION

The P2X7 receptor (P2X7R), a member of the ATP-gated ion channel family, may be a target for the treatment of diseases characterized by inflammation and chronic pain.[1−4] P2X7Rs are expressed in a variety of cell types involved in inflammation and immune system function,[5−7] including mast cells, macrophages, and lymphocytes (T and B).[8] Although its expression in neurons is unclear,[9] P2X7R is expressed in microglia and astrocytes in the central nervous system.[10,11] ATP agonism of P2X7R has been shown to result in rapid changes in intracellular calcium and potassium concentrations, cell maturation, and the release of the pro-inflammatory cytokines IL-1$\beta$ and IL-18 from macrophages and microglia.[12−14] In addition, prolonged exposure of P2X7R to an agonist induces cytolytic pore formation in the plasma membrane, allowing the uptake of fluorescent dyes and EtBr ion, a process that may lead to cell lysis and death.[15,16] Moreover, activation of P2X7R may significantly decrease the uptake of glutamate in astrocytes via the glial-specific glutamate/aspartate transporter (GLAST), suggesting that antagonism of P2X7R may allow GLAST function to recover and protect neurons from excitotoxicity induced by traumatic injury.[11] P2X7R antagonists may be utilized to treat patients with neuropathic pain by inhibiting the release of

cathepsin S, a molecule expressed in spinal microglia that contributes to the maintenance of persistent pain induced by CNS or PNS injury.[17]

Recent studies with $P2X_7$R-knockout (KO) mice clearly indicate that P2X7R is involved in inflammation and chronic pain.[18,19] $P2X_7$R-deficient mice showed a loss of ATP-dependent immune cell functions, including IL-1$\beta$ production and L-selectin shedding, and significant reductions in arthritis symptoms compared with wild type mice.[18] $P2X_7$R-KO mice also showed reduced sensitivity to inflammation and nerve insults,[3,20] in agreement with the efficacy profile of selective P2X7R antagonists in models of chronic inflammation and neuropathic pain.[4,21]

The localization of P2X7R on immune system cells and its pathological roles in immune-related conditions have suggested that this receptor may be a promising target in various disease states and conditions, including chronic inflammation,[22] neurodegeneration,[23,24] ischemia,[25,26] and chronic pain.[27,28] This has led to intensive efforts to identify and develop potent and selective P2X7R antagonists.[22,29−33] Although KN-62
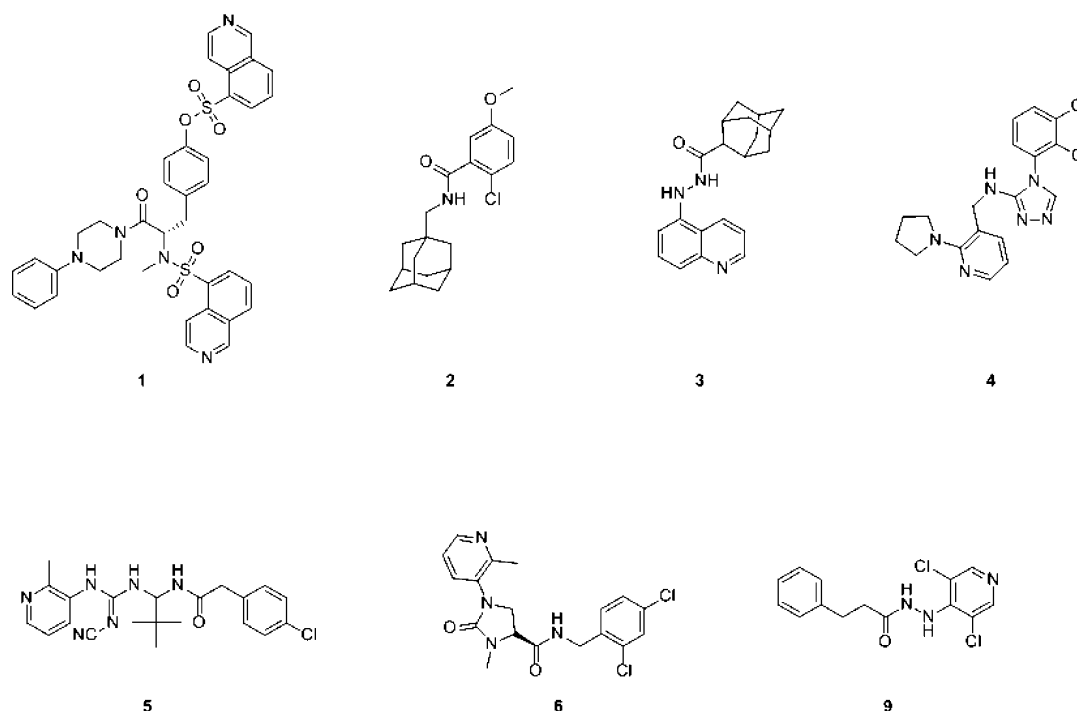
**Figure 1.** The structures of current P2X$_7$R antagonists.

(1-(N,O-bis(1,5-isoquinolinesulfonyl)-N-methyl-L-tyrosyl)-4-phenylpiperazine, **1**) and its derivatives were found to act as selective and potent P2X$_7$R antagonists,[34,35] **1** is poorly soluble in water[36] and has noncompetitive and weak antagonistic activity in rat P2X$_7$R,[37] making **1** unsuitable for use as a drug. AstraZeneca R&D has reported that adamantane-based small molecules (**2**)[38] and a series of cyclic imide moieties[39] act as P2X$_7$R antagonists, and Abbott Laboratories developed N-aryl carbohydrazide (**3**),[40] triazole (**4**),[41] and cyanoguanidine (**5**)[42] as novel antagonists of P2X$_7$R, with substantial improvements in chemical stability, selectivity, and antagonistic activity.[43] Moreover, GlaxoSmithKline recently described an imidazolidine carboxamide (**6**),[44] which had low in vivo clearance and high oral bioavailability in all species examined and appreciable efficacy in rat pain models. Previous studies from our laboratory showed that derivatives of pyrazolodiazepine[29] and 5,6-dihydrodibenzo[a,g]quinolizinium[45] could be characterized as novel P2X$_7$R antagonists.[45]

In an effort to develop new P2X$_7$R antagonists, we assessed the structure−activity relationship (SAR) of a series of pyridinyl hydrazide analogues of compound **9** (IC$_{50}$ = 650 nM, Figure 1), which had been identified as a new P2X$_7$R antagonist by cell-based screening of a representative chemical library (available at Korean Chemical Bank). We also attempted to optimize the biological properties of compound **9** derivatives, including their ability to suppress IL-1$\beta$ production and iNOS/COX-2 induction in BzATP-stimulated THP-1 cells.

## ■ RESULTS AND DISCUSSION

**Chemistry.** The synthetic routes used to prepare compound **9** and its derivatives are shown in three schemes (Schemes 1, 2, and 3). Compound **9** was synthesized from the conventional coupling reaction of hydrocinnamic acid and 3,5-dichloro-4-hydrazinylpyridine (**8**), which had been synthesized by the nucleophilic aromatic substitution of 3,5-dichloro-4-iodopyridine (**7**) by hydrazine (Scheme 1). To explore the SAR of the phenylpropanehydrazide moiety of compound **9**, we
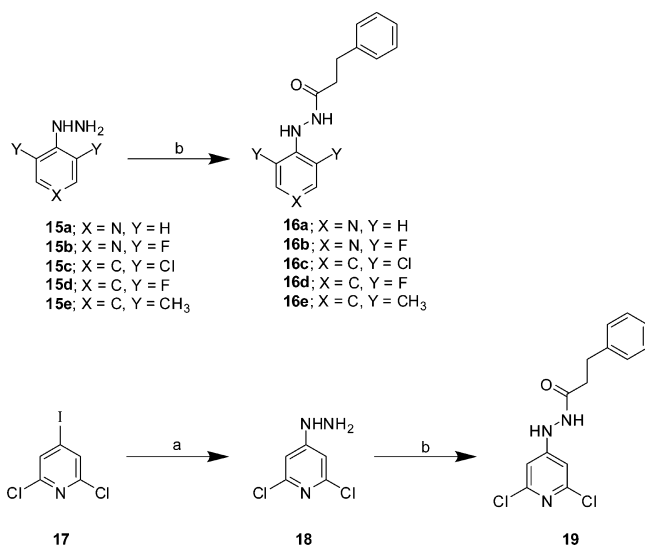
synthesized the modified derivatives, **10**, **12**, and **14** and tested their antagonistic potency at hP2X$_7$R. The N-alkylated compounds **10** and **11** were prepared by reductive alkylation of **8** with phenylpropionaldehyde and formaldehyde, respectively. Acylation of the N-methylated intermediate, **11**, with hydrocinnamoyl chloride yielded compound **12**. An amide derivative, **14**, was synthesized by the reaction between phenylpropionylchloride and 3,5-dichloro-4-aminopyridine for comparison with the hydrazide linker in the lead compound **9** (Scheme 1). Hydrazinyl intermediates (**15a−15e** and **18**) were purchased or prepared from the corresponding halogen substituted compounds using the same procedure used to prepare compound **8** from 3,5-dichloro-4-iodopyridine (**7**). We also made various modifications of the substitutions and the nitrogen of the pyridine in compound **9**. The pyridine analogue **16a**, the 3,5-difluoropyridine analogue **16b**, and the 2,6-dichloropyridine analogue **19** were generated by nucleophilic substitutions of 4-bromo- or 4-iodopyridine derivatives with hydrazine followed by coupling reactions (Scheme 2). Similarly, the phenylhydrazide derivatives, **16c−16e**, instead of pyridine skeleton of **9**, were prepared similarly with 3,5-dichloro, difluoro, and dimethyl substituents (Scheme 2). To modify the acyl group in **9**, the carbamate analogue **34** was synthesized by reacting compound **8** with benzylchloroformate, and the urea analogue **35** was synthesized by reacting benzylamine with the activated form of **8** after treatment with carbonyldiimidazole.

We also synthesized compounds with various aromatic, cycloalkyl, and adamantanyl groups by the substitution of the phenethyl group in compound **9**, via coupling reactions with the hydrazinylpyridine intermediate, **8**, thus optimizing hP2X$_7$R antagonistic potency (Scheme 3).

**Biology.** BzATP-induced pore formation in hP2X$_7$-expressing HEK293 cells is the primary assay used to test the antagonistic effects of the pyridine-4-hydrazide derivatives at hP2X$_7$R, with activity measured as ethidium bromide (EtBr) uptake.[46] **1** was used as the positive control. The SAR at the

**Scheme 1**[a]
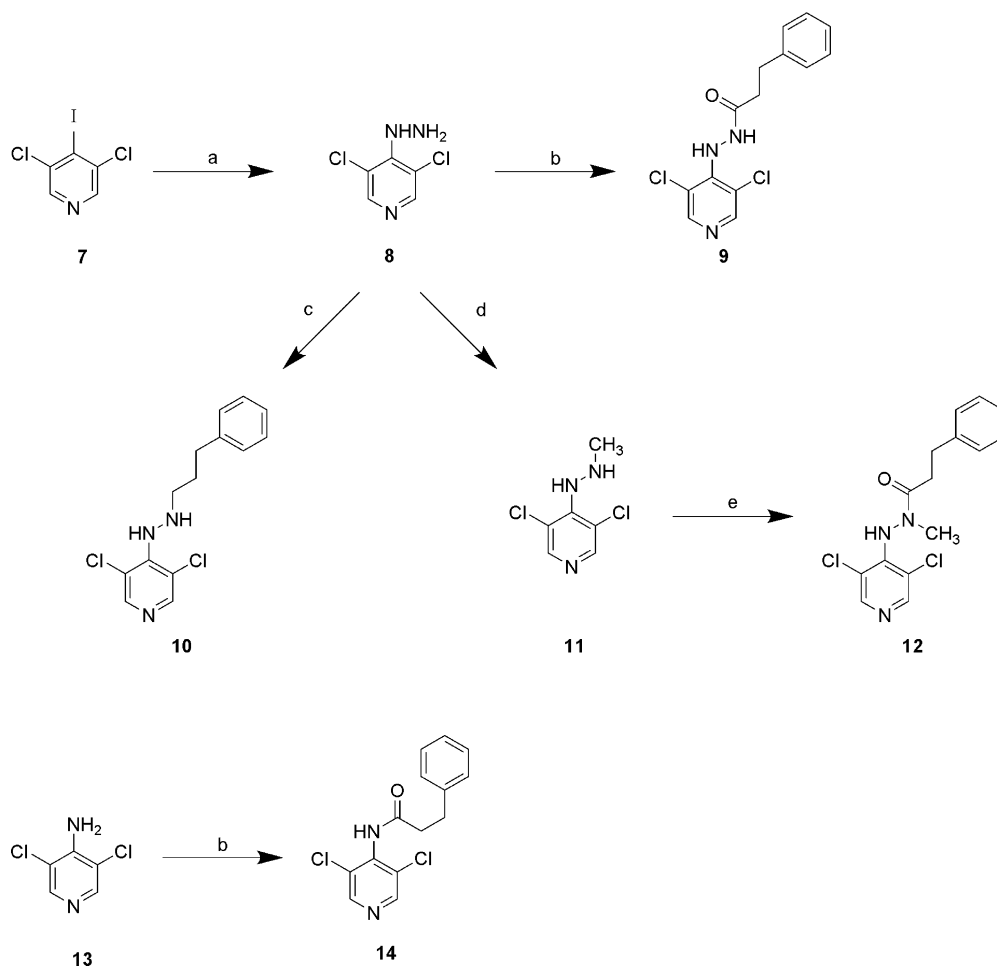


[a]Reagents and conditions: (a) hydrazine hydrate, EtOH, 90 °C, 16 h, 78%; (b) EDC, DIPEA, hydrocinnamic acid, CH$_2$Cl$_2$, RT, 1 h, 88%; (c) 3-phenylpropionaldehyde, NaBH$_3$CN, 1% AcOH in DCE, RT, 2.5 h, 99%; (d) formaldehyde, NaBH$_3$CN, 1% AcOH in DCE, RT, 2.5 h, 80%.

**Scheme 2**[a]



**15a**; X = N, Y = H
**15b**; X = N, Y = F
**15c**; X = C, Y = Cl
**15d**; X = C, Y = F
**15e**; X = C, Y = CH$_3$

**16a**; X = N, Y = H
**16b**; X = N, Y = F
**16c**; X = C, Y = Cl
**16d**; X = C, Y = F
**16e**; X = C, Y = CH$_3$

[a]Reagents and conditions: (a) hydrazine hydrate, n-BuOH, 90−100 °C, 18 h, 50−60%; (b) EDC, DIPEA, hydrocinnamic acid, CH$_2$Cl$_2$, RT, 1 h, 32−94%.

hydrazide linker in the structure of lead compound **9** (IC$_{50}$ = 650 nM) was analyzed by evaluating the activity of the

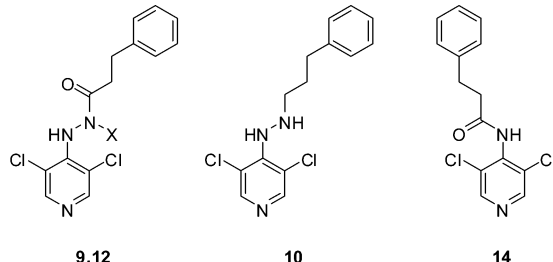**Scheme 3**[a]
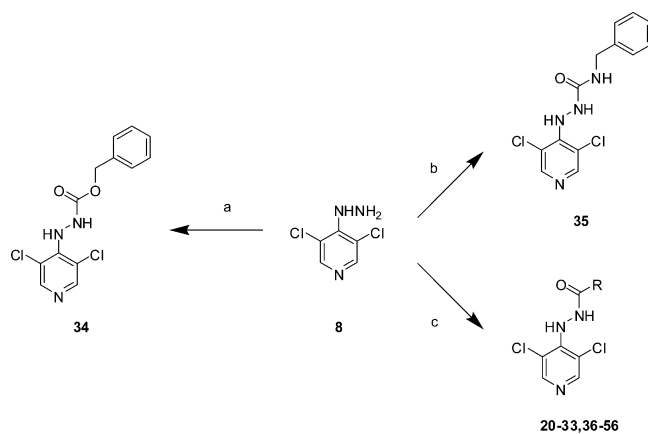


[a]Reagents and conditions: (a) benzyl chloroformate, CH$_2$Cl$_2$, RT, 2 h, 71%; (b) (i) carbonyl diimidazole, TEA, CH$_2$Cl$_2$, RT, 3.5 h, (ii) benzyl amine, TEA, RT, 1 h, 49%; (c) EDC, DIPEA, acid compound, CH$_2$Cl$_2$ or DMF, RT, 1−4 h, 66−94%. (Each structure of R group can be referred from Table 3.)

analogues **10**, **12**, and **14**, in which **9** had been modified with hydrazine, N′-methyl hydrazide, and amide linkers, respectively. We found that all three modified analogues were inactive in hP2X$_7$R antagonism, suggesting that the intact hydrazide linker

is essential and important for the antagonism of compound **9** at hP2X$_7$R (Table 1) and that this hydrazide moiety may

**Table 1. P2X$_7$R Antagonistic Activities of 3,5-Dichloropyridine Derivatives with Modifications of Hydrazide Linker of the Lead Compound 9**
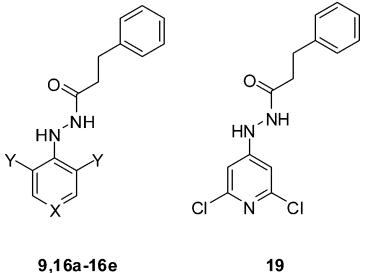


| compd | X | IC$_{50}$ (nM)$^a$ |
|---|---|---|
| 1 | | 280 ± 40 |
| 9 | H | 650 ± 170 |
| 10 | | <20%$^b$ |
| 12 | CH$_3$ | <20%$^b$ |
| 14 | | <20%$^b$ |

$^a$Number of determinations ≥3. $^b$Percent inhibition at concentration 10 $\mu$M and number of determination ≥3.

participate in crucial interactions such as hydrogen bonding with P2X$_7$R.

We also tested the activity of compound **9** derivatives in which the nitrogen of the pyridine ring and dichloride groups had been modified (Table 2). We found that compound **16c**,

**Table 2. P2X$_7$R Antagonistic Activities of Derivatives with Modifications of Dichloropyridine Skeleton of the Lead Compound 9**



| compd | X | Y | IC$_{50}$ (nM)$^a$ |
|---|---|---|---|
| 9 | N | Cl | 650 ± 170 |
| 16a | N | H | <20%$^b$ |
| 16b | N | F | <20%$^b$ |
| 16c | C | Cl | 1400 ± 200 |
| 16d | C | F | <20% |
| 16e | C | CH$_3$ | 900 ± 90 |
| 19 | | | <20%$^b$ |

$^a$Number of determinations ≥3. $^b$Percent inhibition at concentration 10 $\mu$M and number of determination ≥3.

the benzene derivative of **9**, had a 2-fold lower antagonistic activity than **9**, with an IC$_{50}$ value of 1.4 $\mu$M. In contrast, the antagonistic effect of the 3,5-dimethylbenzene derivative **16e** (IC$_{50}$ = 900 nM) was only slightly lower than that of **9**, demonstrating that the benzene ring is tolerated at the receptor. In the analysis of the effect of the 3,5-dichloro substituents of **9**, both the unsubstituted (**16a**) and 2,6-dichloro (**19**) pyridine derivatives of **9** showed significantly reduced antagonistic

activity, indicating that dichlorides and their positions in the pyridine ring are important in the modulation of P2X$_7$R activity. We also found that the 3,5-difluoride derivatives **16b** and **16d**, with relatively smaller halogen isosteres, were totally inactive in the ethidium uptake assay.

Because the antagonistic activity of the 3,5-dimethylbenzene derivative **16e** was comparable to that of compound **9**, certain sized substituents at the 3 and 5 positions of pyridine, such as chloro and methyl groups, may have steric effects on the branched hydrazide moiety, resulting in a conformation favorable to the efficient antagonism of P2X$_7$R. Although none of the modified compounds described above had antagonistic potency greater than that of the lead compound **9**, the initial SAR studies of the linker and skeleton confirmed the importance of the hydrazide linker and positions of the chlorides in the pyridine ring.
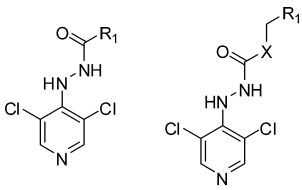
We attempted to optimize the P2X$_7$R antagonism of **9** by modifying its phenethyl group (Tables 3 and 4). We therefore synthesized compounds **20−23**, containing fluoride, chloride, methyl, and methoxy groups, respectively, at the para position, to test the activities of compounds with different substituents. We found that the antagonistic activity of these four derivatives ranged from 0.9 to 1.5 $\mu$M (Table 3). When analyzing the effects of substitutions at 2 positions, we found that the antagonistic activity of the 2,4-dichloro compound **25** was significantly weaker than that of the 4-chloro compound, **24**, suggesting that the presence of multiple substituents on the phenyl group did not favor antagonism. We also found that the incorporation of hydrophilic groups, such as phenol (**26**) and pyridine (**27**) moieties, resulted in a loss of antagonistic potency. These findings indicate that compact and hydrophobic groups are the preferred pharmacophores at this position.
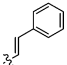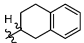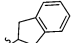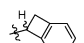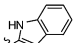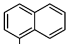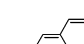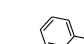
We also attempted to optimize the spatial distance between the phenyl ring and the 3,5-dichloropyridine-4-hydrazide in compound **9** by testing compounds **28−33**, with carbon chains ranging from 0 to 6 in length. We found that the optimum number of carbons was 2, corresponding to the structure of the lead compound **9**. Interestingly, compound **33** with a six-carbon chain showed antagonistic potency with an IC$_{50}$ value of 950 nM, suggesting that more lipophilic groups may be pharmacophores at that position, in addition to the optimized phenethyl group. To test the effects of a hydrogen bond acceptor and donor in place of the $\alpha$-carbon, we assayed the activities of the carbamate analogue, **34**, and the urea analogue, **35**, respectively. Compared with compound **9**, compound **34** showed a nearly 2-fold increase in antagonistic potency at hP2X$_7$R with an IC$_{50}$ value of 370 nM, whereas **35** did not have an antagonistic effect. These results suggest that the presence of an additional hydrogen bond acceptor at the position of the $\alpha$-carbon may play a role in the interaction with hP2X$_7$R.

We also synthesized several conformationally constrained derivatives with restricted free rotation of the phenethyl moiety, containing unsaturated carbon chains and bicyclic ring moieties. In general, constrained analogues with extended forms of aromatic groups, such as the *trans*-cinnamoyl (**36**), (±)-tetrahydronaphthalene (**37**), dihydro-1*H*-indene (**38**), and 2-indole (**40**) derivatives, were inactive or weak P2X$_7$R antagonists. However, the (±)-benzocyclobutyl derivative **39**, possessing a highly compact structure with a bent form of conformation, showed a 2-fold increase in potency, with an IC$_{50}$ value of 320 nM.

When we analyzed the effects of $\pi$−$\pi$ interaction using derivatives with bulkier naphthalene groups (**41−43**), we found that the

## Table 3. P2X$_7$R Antagonistic Activities of 3,5-Dichloropyridine Derivatives with Modifications of Phenylpropanehydrazide Moiety of the Lead Compound 9
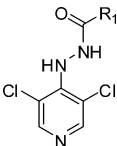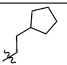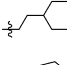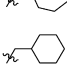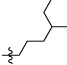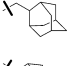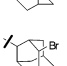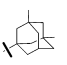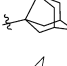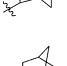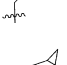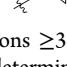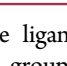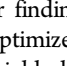


| compd | X | R$_1$ | IC$_{50}$ (nM)[a] |
|---|---|---|---|
| 20 | | 4-F-Ph-(CH$_2$)$_2$- | 900 ± 250 |
| 21 | | 4-Cl-Ph-(CH$_2$)$_2$- | 1,100 ± 100 |
| 22 | | 4-Me-Ph-(CH$_2$)$_2$- | 1,400 ± 200 |
| 23 | | 4-OMe-Ph-(CH$_2$)$_2$- | 1,500 ± 300 |
| 24 | | 4-Cl-Bn- | 620 ± 30 |
| 25 | | 2,4-diCl-Bn- | 2,500 ± 300 |
| 26 | | 4-OH-Ph-(CH$_2$)$_2$- | <20%[b] |
| 27 | | 4-Pyridyl-(CH$_2$)$_2$- | <20%[b] |
| 28 | | Ph- | <20%[b] |
| 29 | | Bz- | 1,100 ± 80 |
| 30 | | Ph-(CH$_2$)$_3$- | 770 ± 60 |
| 31 | | Ph-(CH$_2$)$_4$- | 1,200 ± 200 |
| 32 | | Ph-(CH$_2$)$_5$- | 1,900 ± 70 |
| 33 | | Ph-(CH$_2$)$_6$- | 950 ± 230 |
| 34 | O | Ph- | 370 ± 130 |
| 35 | NH | Ph- | <20%[b] |
| 36 | |  | <20%[b] |
| 37 | |  | 1,100 ± 100 |
| 38 | |  | 4,200 ± 80 |
| 39 | |  | 320 ± 10 |
| 40 | |  | <20%[b] |
| 41 | |  | <20%[b] |
| 42 | |  | <20%[b] |
| 43 | |  | 1,200 ± 200 |

[a]Number of determinations ≥3. [b]Percent inhibition at concentration 10 μM and number of determination ≥3.

## Table 4. P2X$_7$R Antagonistic Activities of 3,5-Dichloropyridine Derivatives with Cycloalkyl and Hydrophobic Rings



| compd | R$_1$ | IC$_{50}$ (nM)[a] |
|---|---|---|
| 44 |  | 380 ± 30 |
| 45 |  | 130 ± 60 |
| 46 |  | 200 ± 40 |
| 47 |  | 730 ± 140 |
| 48 |  | 360 ± 40 |
| 49 |  | 340 ± 40 |
| 50 |  | 77 ± 28 |
| 51 |  | 4.9 ± 0.5 |
| 52 |  | 13 ± 1 |
| 53 |  | 1,400 ± 300 |
| 54 |  | 2,800 ± 500 |
| 55 |  | 210 ± 20 |
| 56 |  | <20%[b] |

[a]Number of determinations ≥3. [b]Percent inhibition at concentration 10 μM and number of determination ≥3.

aromatic group of the ligand and the receptor may not be essential or a bulky R$_1$ group may attenuate binding to P2X$_7$R.

On the basis of our findings with compound **33**, we tested another approach to optimize the antagonistic potency of these compounds by using highly lipophilic groups such as cycloalkyl and adamantanyl at the R$_1$ position (Table 4). Cycloalkyl derivatives with 5-, 6-, and 7-membered rings (compounds **44**–**48**) at the R$_1$ position displayed good antagonistic profile when compared with analogues containing aromatic groups. Several cycloalkyl derivatives showed potent antagonistic activity comparable to or better than those of compounds **1** and **9**, with IC$_{50}$ values ranging from 130 to 380 nM. We found that the cyclohexyl derivative **45** (IC$_{50}$ = 130 nM) was the most potent antagonist among this series of compounds, with a greater than 2-fold increase in antagonistic activity compared with the positive control, compound **1**. Testing of the chain length of this class of compounds (compounds **45**, **47**, and **48**) yielded results similar

antagonistic effect of the 3-(naphthalen-1-yl)propanehydrazide derivative **43** was 2-fold lower, whereas the 2-(naphthalen-1-yl)acetohydrazide derivatives **41** and **42** with shorter carbon chains were inactive. Thus π–π interactions between the

to those of the analogues described in Table 3, with a two-carbon chain being the optimal spacer length between the hydrazide and ring moieties for antagonism. To investigate the effects of more hydrophobic moieties at the $R_1$ position, we synthesized and tested several adamantane, noradamantane, and norbornane analogues (compounds **49−56**). Among this series of poly-cycloalkyl derivatives, the adamantane-based molecules **49−52** were more potent antagonists at hP2X$_7$R than the other compounds **53−56**. Although the potency of the adamantany-lacetohydrazide derivative **49** was not significantly higher than that of compound **9**, the adamantanylhydrazide derivative **50**, which was one carbon shorter, showed enhanced antagonistic potency, with an IC$_{50}$ value of 77 nM. Further optimization of this series yielded the 3-bromoadamantanyl (**51**) and 3,5-dimethyladamantanyl (**52**) derivatives, which had IC$_{50}$ values of 4.9 and 13 nM, respectively. However, other stereoscopic derivatives except for **55** displayed very weak antagonistic activity (**53−56**).

Among the optimized derivatives, compound **52** was further evaluated for its selectivity at the mP2X$_1$ and hP2X$_3$ receptors. Two-electrode voltage clamping (TEVC) experiments were carried out on *Xenopus* oocytes with the overexpression of mP2X$_1$ or hP2X$_3$ receptors by microinjection of corresponding capped ribonucleic acids (cRNA). As a result, 10 $\mu$M **52** showed only 10−20% reduction of the 2 $\mu$M ATP-induced ion current of P2X$_1$ and P2X$_3$ receptors, suggesting high selectivity of the antagonist for P2X$_7$ receptor vs P2X$_1$ and P2X$_3$ receptors. The detailed data was described in the Supporting Information (Figure S1).

IL-1$\beta$ is a major mediator of inflammatory signaling in activated immune system cells in chronic inflammatory diseases and is produced in THP-1 cells by LPS and IFN-$\gamma$-stimulation.[47] Because the activation of P2X$_7$R is an important upstream event for IL-1$\beta$ processing and release following LPS/IFN-$\gamma$ stimulation of THP-1 cells, we tested whether the novel 3,5-dichloropyridine-4-hydrazide analogues with potent antagonistic activity in the EtBr assay could inhibit the release of IL-1$\beta$ by LPS/IFN-$\gamma$/BzATP stimulated THP-1 cells, as determined by ELISA (Table 5). We found that selected

**Table 5. Inhibitory Activities of Selected P2X$_7$R Antagonists against BzATP-Induced IL-1$\beta$ Release in Differentiated THP-1 Cells**

| compd | IC$_{50}$ (nM)[a] | | compd | IC$_{50}$ (nM)[a] | |
| | EtBr assay | IL-1$\beta$ | | EtBr assay | IL-1$\beta$ |
|---|---|---|---|---|---|
| **1** | 280 ± 40 | 120 ± 20 | **46** | 200 ± 40 | 42 ± 13 |
| **9** | 650 ± 170 | 320 ± 120 | **50** | 77 ± 28 | 130 ± 20 |
| **34** | 370 ± 130 | 20%[b] | **51** | 4.9 ± 0.5 | 1.3 ± 0.4 |
| **39** | 320 ± 10 | 13%[b] | **52** | 13 ± 1 | 9.2 ± 2.4 |
| **45** | 130 ± 60 | 56 ± 11 | | | |

[a]Number of determinations ≥3. [b]Percent inhibition at concentration 10 $\mu$M and number of determination ≥3.

derivatives with IC$_{50}$ values in submicromolar ranges in the EtBr assay showed generally parallel order of potency of inhibition in the assay of IL-1$\beta$ production, except for **34** and **39**. Especially, the adamantane-based derivatives (**50−52**) significantly in-hibited the release of IL-1$\beta$, with IC$_{50}$ values in the range of 1.3−130 nM, while the range of IC$_{50}$ values in the EtBr assay was 4.9−77 nM. Thus, the potent antagonists we synthesized were confirmed as having functional activity in modulating inflammatory signals mediated by the activation of P2X$_7$R.

Excess nitric oxide (NO) produced by iNOS is an important mediator of acute and chronic inflammation.[48] COX-2, which is induced by LPS or a mixture of several cytokines, is also involved in the pathology of chronic inflammation.[49] To test whether derivative **52** suppresses the expression of inflamma-tory proteins, we tested its effect on BzATP-stimulated iNOS and COX-2 expression in THP-1 cells. Western blot analyses showed that exposure of THP-1 cells to LPS/IFN-$\gamma$ slightly increased cellular levels of iNOS and COX-2 proteins and that BzATP treatment potentiated the expression of both (Figure. 2A). However, compound **52**, at a concentration of
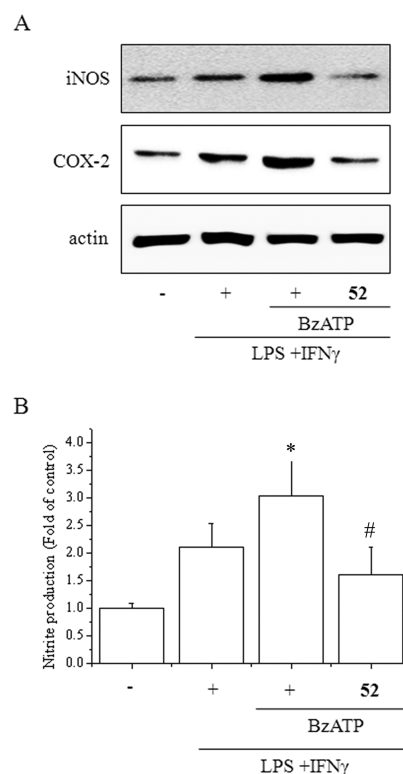


**Figure 2.** Inhibition of iNOS and COX-2 expression by **52**. Effects of **52** on (A) protein expression of iNOS/COX-2 and (B) NO production. For the differentiation into macrophage phenotype, THP-1 cells were exposed to 25 ng/mL LPS and 10 ng/mL IFN$\gamma$ for 3 h and the differentiated cells were incubated with **52** for 30 min and then incubated with 1 mM BzATP for an additional 24 h. Total cell lysates were subjected to immunoblottings for the detection of iNOS and COX-2. Culture media were used for the detection of medium nitrite levels. Data represents means ± SD with 4 different samples (significant versus LPS/IFN-$\gamma$-treated group, *$p < 0.05$; signi-ficant versus LPS/IFN-$\gamma$ + BzATP-treated group, #$p < 0.05$).

1 $\mu$M, almost completely reduced iNOS and COX-2 protein expression in response to P2X$_7$R activation (Figure 2A), showing that **52** efficiently suppresses the de novo synthesis of the inflammatory proteins, iNOS and COX-2. The previous literature reported that the activation of P2X$_7$ receptor enhances interferon-$\gamma$ (IFN$\gamma$)-induced type II nitric oxide synthase activity in BV-2 microglial cells and the IFN$\gamma$-induced NO production was suppressed by nonselective P2X antagonists including suramine and oxidized ATP (oxATP).[50] Another report suggested that the action of P2X$_7$R receptor was related with the regulation of downstream transcription factor, FosB/AP-1, in multiple cell types including the role of nucleotide-induced COX-2 expression in murine astrocytes.[49]

Therefore, we suggested that compound **52** may attenuate the production of iNOS/COX-2 in activated THP-1 cells through P2X$_7$R receptor antagonism and subsequent regulation of the downstream signaling pathway. To assess whether the inhibition of iNOS expression by compound **52** reduces NO production, we further evaluated nitrite concentrations in the culture media. As a result, the accumulation of nitrite in the culture media by addition of BzATP to THP-1 cells primed with LPS/IFN-γ significantly attenuated by 1 μM compound **52** (Figure 2B), confirming that compound **52** efficiently suppresses the NO production mediated by P2X$_7$R activation and LPS induction in macrophages.

These results suggest that the novel P2X$_7$R antagonists developed in this study may be useful as therapeutic agents for inflammatory disorders related with the upregulation of iNOS/COX-2 such as NO-mediated inflammatory bowel disease[51] (IBD) and others.[52,53]

## ■ CONCLUSIONS

Conventional screening for P2X$_7$R antagonists using the ethidium bromide uptake assay led to the identification of the 3,5-dichloropyridine analogue, **9**, as the lead compound. To optimize P2X$_7$R antagonistic potency, we tested the effects of modifications at the hydrazide, dichloropyridine, and phenylethyl groups of **9**. SAR analysis suggested that (1) the hydrazide linker was essential, (2) dichloro-substitution at the 3- and 5-positions of the pyridine was favorable for the antagonism of P2X$_7$R activity, (3) two-carbon chain between the phenyl ring and 3,5-dichloropyridine-4-hydrazide was the optimal spatial distance, (4) a hydrogen bond acceptor at the α-carbon (**34**) enhanced P2X$_7$R antagonism, and (5) derivatives (**50−52**) with compact hydrophobic adamantane groups instead of phenyl group showed optimum antagonism. The potent antagonists also showed parallel activities for the inhibition of IL-1β release from differentiated THP-1 cells. Especially, derivative **52** was highly selective for hP2X$_7$ receptor vs mP2X$_1$ and hP2X$_3$ receptors and significantly suppressed the expression of inflammatory proteins such as COX-2 and iNOS in LPS/IFN-γ/BzATP-stimulated THP-1 cells. These P2X$_7$R functional assays indicate that 3,5-dichloropyridine-based P2X$_7$R antagonists may hold promise in the treatment of inflammatory disorders.

## ■ EXPERIMENTAL SECTION

**Chemistry.** Reagents and solvents were purchased from commercial suppliers and used without further purification. $^1$H and $^{13}$C NMR spectra were determined with a JEOL JNM-LA 300WB spectrometer at 300 MHz or JEOL JNM-ECX 400P spectrometer at 400 MHz, and spectra were taken in CDCl$_3$ or DMSO-$d_6$. Unless otherwise noted, chemical shifts are expressed as δ units (ppm) downfield from internal tetramethylsilane or relative ppm from DMSO (2.5 ppm) and coupling constants (*J*) are in Hertz (Hz). Mass spectroscopy was performed on ESI. Melting points were determined in open capillary tubes using a Stuart melting point apparatus SMP10. The purity of compounds was determined by elemental analysis, carried out with an elemental analyzer (Flash EA 1112series/CE Instruments). All compounds tested in the biological assay showed more than 95% purity unless noted.

*Preparation of 3,5-Dichloro-4-hydrazinylpyridine (8).* 3,5-Dichloro 4-iodopyridine (**7**, 1.0 g, 3.6 mmol) and hydrazine hydrate (540 μL, 18.0 mmol) were dissolved in ethanol (20 mL). The reaction mixture was refluxed for 16 h. The reaction solution was dried by rotary evaporator. The residue was taken up in saturated aqueous NaHCO$_3$ solution and extracted with ethyl acetate (2×). The combined extracts were dried over sodium sulfate, filtered, and evaporated. The residue was purified by silica gel column chromatography (CH$_3$Cl:methanol =

40:1) to give hydrazine intermediate **8** (500 mg, 78%). $^1$H NMR (CDCl$_3$, 300 MHz): δ 8.24 (2H, s), 6.10 (1H, s), 4.16 (2H, s). ESI [M − H] = 177.0.

*General Procedure for the Preparation of Hydrazide Compounds Using Coupling Reaction.* Intermediate **8** (1 equiv) was dissolved in anhydrous dichloromethane, followed by addition of acidic compound (1.5 equiv), 1-ethyl-3-[3-dimethylaminopropyl]carbodiimide hydrochloride (EDC, 1.5 equiv), and diisopropylethylamine (1.5 equiv). The reaction mixture was stirred for 30−90 min at room temperature. The solvent was removed by rotary evaporator. The residue was taken up in saturated aqueous NaHCO$_3$ solution and extracted with ethyl acetate (2×). The combined organic later was dried over sodium sulfate, filtered, and evaporated. The residue was purified by silica gel column chromatography to give tested compounds. (**9**, **14**, **16a**, **16c−16e**, **19−34**, **36−56**).

*N′-(3,5-Dichloropyridin-4-yl)-3-phenylpropanehydrazide (9).* Following the general procedure using **8** and hydrocinnamic acid, **9** was obtained as a white solid (30.8 mg, 88%); mp 149−151 °C. $^1$H NMR (CDCl$_3$, 300 MHz): δ 8.28 (2H, s), 7.61 (1H, d, *J* = 3.3 Hz, N−H), 7.31−6.83 (5H, m), 6.82 (1H, d, *J* = 3.9 Hz, N−H), 2.97 (2H, t, *J* = 7.7 Hz), 2.55 (2H, t, *J* = 7.5 Hz). $^{13}$C NMR (CDCl$_3$, 300 MHz): δ 172.9, 154.1, 143.0, 137.1, 136.5, 134.9, 124.6, 120.9, 37.3, 31.2. ESI [M + H] = 311.9.

*3,5-Dichloro-4-(2-(3-phenylpropyl)hydrazinyl)pyridine (10).* 3,5-Dichloro-4-hydrazinylpyridine (**8**, 40.0 mg, 0.2 mmol) and 3-phenylpropionaldehyde (40.0 μL, 0.3 mmol) were dissolved in 0.1% acetic acid of anhydrous 1,2-dichloroethane (2.0 mL). The reaction mixture was stirred at room temperature for 30 min. Sodium cyanoborohydride (18.0 mg, 0.3 mmol) was added in the mixture and stirred at room temperature for 2 h. Brine (10.0 mL) was added to quench the reaction, and the mixture was transferred to a separatory funnel and then extracted with dichloromethane (2×). The combined organic layer was dried over sodium sulfate, filtered, and evaporated. The residue was purified by silica gel column chromatography to give **10** as a sticky oil (66.1 mg, 99%). $^1$H NMR (CDCl$_3$, 400 MHz): δ 8.22 (2H, s), 7.28−7.14 (5H, m), 6.09 (1H, s, N−H), 4.31 (1H, d, *J* = 4.8 Hz, N−H), 2.83−2.78 (2H, m), 2.66 (2H, t, *J* = 7.8 Hz), 1.81−1.74 (2H, m). $^{13}$C NMR (CDCl$_3$, 400 MHz): δ 154.5, 152.6, 147.3, 132.9, 132.8, 130.2, 122.6, 48.8, 29.0, 24.3. ESI [M + H] = 297.3.

*N′-(3,5-Dichloropyridin-4-yl)-N-methyl-3-phenylpropanehydrazide (12).* 3,5-Dichloro-4-hydrazinylpyridine (**8**, 50.0 mg, 0.3 mmol) and formaldehyde (14.0 μL, 0.4 mmol) were dissolved in 1% acetic acid of anhydrous 1,2-dichloroethane (2.0 mL). The reaction mixture stirred at room temperature for 30 min. Sodium cyanoborohydride (27.0 mg, 0.4 mmol) was added in the mixture and stirred at room temperature for 2 h. Brine (10.0 mL) was added to quench the reaction, and the mixture was transferred to a separatory funnel and then extracted with dichloromethane (2×). The combined organic layer was dried over sodium sulfate, filtered, and evaporated. The residue was purified by silica gel column chromatography to give **11** as a white solid (28.4 mg, 52%). Following the general procedure using the **11** and hydrocinnamic acid, **12** was obtained as a white solid (39.2 mg, 80%); mp 113−115 °C. $^1$H NMR (CDCl$_3$, 400 MHz): δ 8.28 (2H, s), 7.31−7.18 (5H, m), 6.49 (1H, s, N−H), 3.06 (3H, s), 2.98 (2H, t, *J* = 7.4 Hz), 2.67 (2H, t, *J* = 7.8 Hz). $^{13}$C NMR (CDCl$_3$, 400 MHz): δ 194.0, 153.8, 151.5, 149.7, 135.6, 135.5, 133.0, 123.3, 20.1, 18.9, 14.0. ESI [M + H] = 325.8.

*N-(3,5-Dichloropyridin-4-yl)-3-phenylpropanamide (14).* Following the general procedure using the 4-amino-3,5-dichloropyridine (**13**) and hydrocinnamic acid, **14** was obtained as a light-yellow gel (21.6 mg, 93%). $^1$H NMR (CDCl$_3$, 400 MHz): δ 8.63 (2H, S), 7.30−7.17 (5H, m), 2.98 (2H, t, *J* = 7.6 Hz), 2.85 (2H, t, *J* = 7.4 Hz). $^{13}$C NMR (CDCl$_3$, 400 MHz): δ 172.5, 156.3, 148.9, 142.2, 140.0, 132.1, 128.5, 126.3, 39.3, 30.2. ESI [M + H] = 296.0.

*3-Phenyl-N′-(pyridin-4-yl)propanehydrazide (16a).* Following the general procedure using the 4-hydrazinypyridine (**15a**, purchased from Sigma Aldrich) and hydrocinnamic acid, **16a** was obtained as a white solid (19.8 mg, 33%); mp 186−188 °C. $^1$H NMR (CDCl$_3$, 400 MHz): δ 7.94 (2H, d, *J* = 5.7 Hz), 7.66 (1H, s, N−H), 7.41−7.15 (5H, m), 6.83 (2H, d, *J* = 5.7 Hz), 6.67 (1H, s, N−H), 2.95 (2H, t, *J* = 7.7 Hz), 2.49

(2H, t, *J* = 7.8 Hz). ^{13}C NMR (CDCl$_3$, 400 MHz): $\delta$ 176.2, 156.1, 151.9, 142.6, 133.5, 130.0, 125.4, 119.8, 36.2, 28.2. ESI [M + H] = 242.1.

*N'-(3,5-Difluoropyridin-4-yl)-3-phenylpropanehydrazide (16b).* 4-Chloro-3,5-difluoropyridine (300 mg, 2.0 mmol) and hydrazine hydrate (380 $\mu$L, 8.0 mmol) were dissolved in ethanol (20 mL). The reaction mixture was refluxed for 14 h. The reaction solution was dried by rotary evaporator. The residue was taken up in saturated aqueous NaHCO$_3$ solution and extracted with ethyl acetate (2×). The combined organic layer was dried over sodium sulfate, filtered, and evaporated. The residue was purified by silica gel column chromatography (CH$_3$Cl:methanol = 50:1) to give hydrazine intermediate **15b** as a pink solid (143 mg, 49%). ^{1}H NMR (CDCl$_3$, 300 MHz): $\delta$ 8.14 (2H, s), 6.39 (1H, s), 4.21 (2H, s). ESI [M − H] = 144.2. Next, following the general procedure using the hydrazine intermediate (**15b**) and hydrocinnamic acid, **16b** was obtained as a sticky oil (26.8 mg, 51%). ^{1}H NMR (CDCl$_3$, 400 MHz): $\delta$ 8.15 (2H, s), 7.36 (1H, s, N−H), 7.30−7.16 (5H, m), 6.39 (1H, s, N−H), 2.97 (2H, t, *J* = 7.6 Hz), 2.53 (2H, t, *J* = 7.4 Hz). ^{13}C NMR (CDCl$_3$, 300 MHz): $\delta$ 180.5, 165.3 (d, *J* = 1062.4 Hz), 143.0, 135.2, 133.4, 128.2, 124.6, 113.7, 29.8, 25.7. ESI [M + H] = 278.0.

*N'-(2,6-Dichlorophenyl)-3-phenylpropanehydrazide (16c).* Following the general procedure using the (2,6-dichlorophenyl)hydrazine (**15c**, purchased from Sigma Aldrich) and hydrocinnamic acid, **16c** was obtained as a transparent oil (25.1 mg, 83%). ^{1}H NMR (CDCl$_3$, 300 MHz): $\delta$ 7.57 (1H, d, *J* = 4.8 Hz, N−H), 7.29−7.14 (7H, m), 6.91 (1H, t, *J* = 8.1 Hz), 6.80 (1H, d, *J* = 5.1 Hz, N−H), 2.95 (2H, t, *J* = 7.7 Hz), 2.49 (2H, t, *J* = 7.8 Hz). ^{13}C NMR (CDCl$_3$, 300 MHz): $\delta$ 180.0, 147.0, 146.3, 133.8, 133.5, 133.1, 131.0, 130.6, 128.5, 32.1, 27.1. ESI [M + H] = 311.0.

*N'-(2,6-Difluorophenyl)-3-phenylpropanehydrazide (16d).* Following the general procedure using the (2,6-fluorophenyl)hydarzine (**15d**, purchased from Apolloscientific) and hydrocinnamic acid, **16d** was obtained as a light-pink solid (30.7 mg, 94%); mp 119−121 °C. ^{1}H NMR (CDCl$_3$, 400 MHz): $\delta$ 7.59 (1H, d, *J* = 5.2 Hz, N−H), 7.29−7.16 (5H, m), 6.91−6.81 (3H, m), 6.41−6.39 (1H, m), 2.96 (2H, t, *J* = 7.8 Hz), 2.48 (2H, t, *J* = 7.8 Hz). ^{13}C NMR (CDCl$_3$, 400 MHz): $\delta$ 180.5, 161.3, 146.4, 133.4, 133.2, 131.1, 126.6, 115.1, 111.7, 32.3, 27.2. ESI [M + H] = 278.0. Purity: 92%.

*N'-(2,6-Dimethylphenyl)-3-phenylpropanehydrazide (16e).* Following the general procedure using the (2,6-dimethylphenyl)hydarzine (**15e**, purchased from Apolloscientific) and hydrocinnamic acid, **16e** was obtained as a gel (31.9 mg, 93%); mp 78−80 °C. ^{1}H NMR (CDCl$_3$, 400 MHz): $\delta$ 7.26−7.11 (6H, m), 6.96 (2H, d, *J* = 7.2 Hz), 6.90−6.86 (1H, m), 6.09 (1H, d, *J* = 3.6 Hz, N−H), 2.93 (2H, d, *J* = 7.6 Hz), 2.42 (2H, d, *J* = 7.6 Hz), 2.31 (3H, s). ^{13}C NMR (CDCl$_3$, 400 MHz): $\delta$ 178.0, 149.8, 146.2, 133.6, 133.2, 132.9, 130.8, 127.7, 32.3, 27.1, 13.0. ESI [M + H] = 268.9.

*N'-(2,6-Dichloropyridin-4-yl)-3-phenylpropanehydrazide (19).* 2,6-Dichloro-4-iodopyridine (**17**, 300 mg, 1.1 mmol) and hydrazine hydrate (175 $\mu$L, 5.5 mmol) were dissolved in ethanol (20 mL). The reaction mixture was refluxed for 16 h. The reaction solution was dried by rotary evaporator. The residue was taken up in saturated aqueous NaHCO$_3$ solution and extracted with ethyl acetate (2×). The combined organic layer was dried over sodium sulfate, filtered, and evaporated. The residue was purified by silica gel column chromatography (CH$_3$Cl:methanol = 45:1) to give hydrazine intermediate **18** as a white solid (186 mg, 57%). ^{1}H NMR (CDCl$_3$, 300 MHz): $\delta$ 6.85 (2H, s), 6.50 (1H, s), 4.78 (2H, s). ESI [M − H] = 177.2. Next, following the general procedure using the hydrazine intermediate **18** and hydrocinnamic acid, **19** was obtained as a white solid (20.6 mg, 71%); mp 154−156 °C. ^{1}H NMR (CDCl$_3$, 300 MHz): $\delta$ 7.36−7.21 (5H, m), 6.99 (1H, s, N−H), 6.45 (2H, s), 6.34 (1H, s, N−H). ^{13}C NMR (CDCl$_3$, 300 MHz): $\delta$ 177.9, 152.8, 151.2, 143.8, 131.3, 130.9, 129.0, 122.3, 35.7, 29.5. ESI [M + H] = 312.0.

*N'-(3,5-Dichloropyridin-4-yl)-3-(4-fluorophenyl)-propanehydrazide (20).* Following the general procedure using the **8** and 4-fluorophenylpropionic acid, **20** was obtained as a white solid (18.4 mg, 84%); mp 182−184 °C. ^{1}H NMR (CDCl$_3$, 400 MHz): $\delta$ 8.28 (2H, s), 7.58 (1H, d, *J* = 3.6 Hz, N−H), 7.12−7.09 (2H, m), 6.96−6.92 (2H, m), 6.80 (1H, d, *J* = 4.0 Hz, N−H), 2.93 (2H, t, *J* =

7.4 Hz), 2.50 (2H, t, *J* = 7.6 Hz). ^{13}C NMR (CDCl$_3$, 400 MHz): $\delta$ 178.2, 168.5, 152.5, 151.3, 139.3, 132.5, 121.9, 116.9, 29.3, 23.7. ESI [M + H] = 328.9.

*3-(4-Chlorophenyl)-N'-(3,5-dichloropyridin-4-yl)-propanehydrazide (21).* Following the general procedure using the **8** and 4-chloroophenylpropionic acid, **21** was obtained as a white solid (28.0 mg, 86%); mp 172−174 °C. ^{1}H NMR (CDCl$_3$, 400 MHz): $\delta$ 8.29 (2H, s), 7.46 (1H, d, *J* = 4.0 Hz, N−H), 7.22 (2H, d, *J* = 8.4 Hz), 7.08 (2H, d, *J* = 8.8 Hz), 6.80 (1H, d, *J* = 4.0 Hz, N−H), 2.93 (2H, t, *J* = 7.4 Hz), 2.50 (2H, t, *J* = 7.4 Hz). ^{13}C NMR (CDCl$_3$, 400 MHz): $\delta$ 171.5, 148.0, 146.9, 138.6, 132.1, 129.6, 128.5, 119.9, 34.7, 30.1. ESI [M + H] = 346.9.

*N'-(3,5-Dichloropyridin-4-yl)-3-p-tolylpropanehydrazide (22).* Following the general procedure using the **8** and 4-toluylpropionic acid, **22** was obtained as a white solid (22.6 mg, 90%); mp 185−187 °C. ^{1}H NMR (CDCl$_3$, 400 MHz): $\delta$ 8.28 (2H, s), 7.51 (1H, d, *J* = 3.6 Hz, N−H), 7.10−7.04 (4H, m), 6.82 (1H, d, *J* = 4.0 Hz, N−H), 2.92 (2H, t, *J* = 7.8 Hz), 2.51 (2H, t, *J* = 7.6 Hz), 2.31 (3H, s). ^{13}C NMR (CDCl$_3$, 400 MHz): $\delta$ 176.6, 152.3, 148.3, 146.2, 138.1, 129.3, 128.1, 120.5, 35.5, 30.4, 21.0. ESI [M + H] = 326.0.

*N'-(3,5-Dichloropyridin-4-yl)-3-(4-methoxyphenyl)-propanehydrazide (23).* Following the general procedure using the **8** and 4-methoxyphenylpropionic acid, **23** was obtained as a white solid (27.9 mg, 90%); mp 148−150 °C. ^{1}H NMR (CDCl$_3$, 400 MHz): $\delta$ 8.28 (2H, s), 7.52 (1H, d, *J* = 4.0 Hz, N−H), 7.07 (2H, d, *J* = 6.4 Hz), 6.80 (2H, d, *J* = 6.4 Hz, N−H), 2.90 (2H, t, *J* = 7.6 Hz), 2.50 (2H, t, *J* = 7.6 Hz). ^{13}C NMR (CDCl$_3$, 400 MHz): $\delta$ 171.7, 158.5, 148.6, 147.1, 132.4, 129.5, 120.7, 114.3, 55.6, 35.9, 30.3. ESI [M + H] = 342.0.

*2-(4-Chlorophenyl)-N'-(3,5-dichloropyridin-4-yl)acetohydrazide (24).* Following the general procedure using the **8** and 4-chlorophenylacetic acid, **24** was obtained as a white solid (30.3 mg, 86%); mp 178−180 °C. ^{1}H NMR (CDCl$_3$, 400 MHz): $\delta$ 8.29 (2H, s), 7.63 (1H, bs), 7.33−7.24 (4H, m), 6.79 (1H, s, N−H), 3.59 (2H, s). ^{13}C NMR (CDCl$_3$, 400 MHz): $\delta$ 175.8, 154.3, 146.1, 139.6, 135.3, 132.8, 126.1, 120.7, 36.9. ESI [M + H] = 332.0.

*2-(2,4-Dichlorophenyl)-N'-(3,5-dichloropyridin-4-yl)-acetohydrazide (25).* Following the general procedure using the **8** and 2,4-dichlorophenylacetic acid, **25** was obtained as a white solid (20.3 mg, 77%); mp 191−193 °C. ^{1}H NMR (CDCl$_3$, 400 MHz): $\delta$ 8.29 (2H, s), 7.51 (1H, d, *J* = 4.0 Hz, N−H), 7.37 (1H, d, *J* = 1.6 Hz), 7.09 (2H, d, *J* = 1.6 Hz), 6.79 (1H, d, *J* = 4.0 Hz, N−H), 3.03(2H, d, *J* = 7.4 Hz), 2.53 (2H, d, *J* = 7.4 Hz). ^{13}C NMR (CDCl$_3$, 400 MHz): $\delta$ 177.6, 152.6, 151.3, 139.6, 137.6, 136.1, 133.8, 132.1, 129.8, 122.2, 37.5. ESI [M + H] = 366.0.

*N'-(3,5-Dichloropyridin-4-yl)-3-(4-hydroxyphenyl)-propanehydrazide (26).* Following the general procedure using the **8** and 4-hydroxyphenylpropionic acid, **26** was obtained as a light-yellow solid (29.6 mg, 93%); mp 154−156 °C. ^{1}H NMR (CDCl$_3$, 400 MHz, $\delta$ ppm, *J* in Hz): $\delta$ 10.12 (1H, s, O−H), 9.14 (1H, s, N−H), 8.20 (2H, s), 8.14 (1H, s, N−H), 6.95 (2H, d, *J* = 8.4 Hz), 6.62 (2H, d, *J* = 8.0 Hz), 2.67 (2H, t, *J* = 7.8 Hz), 2.35 (2H, t, *J* = 7.8 Hz). ^{13}C NMR (CDCl$_3$, 400 MHz): $\delta$ 177.8, 161.1, 153.0, 151.6, 134.4, 132.3, 119.2, 117.0, 29.3, 23.8. ESI [M + H] = 328.0.

*N'-(3,5-Dichloropyridin-4-yl)-2-(pyridin-4-yl)acetohydrazide (27).* Following the general procedure using the **8** and 3-(pyridin-4-yl)propanoic acid, **27** was obtained as a white solid (27.7 mg, 92%); mp 220−222 °C. ^{1}H NMR (CDCl$_3$, 400 MHz): $\delta$ 8.59 (2H, d, *J* = 5.6 Hz), 8.30 (2H, s), 7.68 (1H, s, N−H), 7.23 (2H, d, *J* = 6.0 Hz), 6.82 (1H, d, *J* = 3.2 Hz, N−H), 3.59 (2H, s). ^{13}C NMR (CDCl$_3$, 400 MHz): $\delta$ 177.3, 155.8, 154.5, 153.2, 149.6, 129.2, 123.6, 36.0. ESI [M + H] = 299.0.

*N'-(3,5-Dichloropyridin-4-yl)benzohydrazide (28).* Following the general procedure using the **8** and benzoic acid, **28** was obtained as a white solid (25.4 mg, 90%); mp 160−162 °C. ^{1}H NMR (CDCl$_3$, 400 MHz): $\delta$ 9.00 (1H, s, N−H), 8.27 (2H, S), 7.80 (2H, d, *J* = 7.2 Hz), 7.54 (1H, t, *J* = 7.6 Hz), 7.44 (2H, t, *J* = 7.6 Hz), 7.07 (1H, s, N−H). ^{13}C NMR (CDCl$_3$, 400 MHz): $\delta$ 171.4, 148.2, 147.1, 132.5, 131.3, 128.8, 127.3, 120.4. ESI [M + H] = 283.9. Purity: 92%.

*N'-(3,5-Dichloropyridin-4-yl)-2-phenylacetohydrazide (29).* Following the general procedure using the **8** and phenylacetic acid, **29** was

obtained as a white solid (21.2 mg, 78%); mp 216−218 °C. $^1$H NMR (CDCl$_3$, 400 MHz): δ 8.24 (2H, s), 7.96 (1H, s, N−H), 7.38−7.27 (5H, m), 6.80 (1H, s, N−H), 3.59 (2H, s). $^{13}$C NMR (CDCl$_3$, 400 MHz): δ 167.9, 146.3, 145.3, 132.2, 128.4, 127.9, 126.6, 119.3, 43.1. ESI [M + H] = 298.0.

*N′-(3,5-Dichloropyridin-4-yl)-4-phenylbutanehydrazide (30).* Following the general procedure using the **8** and phenylbutanoic acid, **30** was obtained as a white solid (29.8 mg, 91%); mp 117−119 °C. $^1$H NMR (CDCl$_3$, 400 MHz): δ 8.30 (2H, s), 7.51 (1H, d, J = 4.0 Hz, N−H), 7.30−7.15 (5H, m), 6.81 (1H, d, J = 4.4 Hz, N−H), 2.65 (2H, t, J = 7.4 Hz), 2.22 (2H, t, J = 7.4 Hz), 2.02−1.95 (2H, m). $^{13}$C NMR (CDCl$_3$, 400 MHz): δ 178.6, 152.9, 151.3, 144.8, 131.2, 131.0, 128.6, 122.2, 29.2, 26.6, 19.6. ESI [M + H] = 325.9.

*N′-(3,5-Dichloropyridin-4-yl)-5-phenylpentanehydrazide (31).* Following the general procedure using the **8** and phenylpentanoic acid, **31** was obtained as a white solid (28.2 mg, 81%); mp 118−120 °C. $^1$H NMR (CDCl$_3$, 400 MHz): δ 8.30 (2H, s), 7.49 (1H, d, J = 4.0 Hz, N−H), 7.29−7.14 (5H, m), 6.83 (1H, d, J = 3.6 Hz, N−H), 2.61 (2H, t, J = 7.2 Hz), 2.23 (2H, t, J = 7.2 Hz), 1.69−1.62 (4H, m). $^{13}$C NMR (CDCl$_3$, 400 MHz): δ 193.7, 164.6, 162.8, 156.6, 141.0, 140.0, 136.9, 130.1, 25.8, 23.1, 20.1, 12.3. ESI [M − H] = 337.7.

*N′-(3,5-Dichloropyridin-4-yl)-6-phenylhexanehydrazide (32).* Following the general procedure using the **8** and phenylhexanoic acid, **32** was obtained as a white solid (27.6 mg, 71%); mp 128−130 °C. $^1$H NMR (CDCl$_3$, 400 MHz): δ 8.29 (2H, s), 7.71 (1H, d, J = 2.4 Hz, N−H), 7.28−7.25 (2H, m), 7.19−7.14 (3H, m), 6.83 (1H, d, J = 3.2 Hz, N−H), 2.58 (2H, t, J = 7.6 Hz), 2.21 (2H, t, J = 7.4 Hz), 1.68−1.61 (4H, m), 1.38−1.24 (2H, m). $^{13}$C NMR (CDCl$_3$, 400 MHz): δ 180.4, 154.3, 152.8, 147.8, 132.5, 129.6, 129.5, 123.7, 31.4, 28.9, 26.4, 23.9, 19.5. ESI [M + H] = 353.3.

*N′-(3,5-Dichloropyridin-4-yl)-7-phenylheptanehydrazide (33).* Following the general procedure using the **8** and phenylheptanoic acid, **33** was obtained as a white solid (31.6 mg, 81%); mp 131−133 °C. $^1$H NMR (CDCl$_3$, 400 MHz): δ 8.29 (2H, s), 7.77 (1H, s, N−H), 7.28−7.24 (2H, m), 7.18−7.14 (3H, m), 6.83 (1H, d, J = 2.8 Hz, N−H), 2.57 (2H, t, J = 7.6 Hz), 2.20 (2H, t, J = 7.6 Hz), 1.64−1.57 (4H, m), 1.33−1.31 (4H, m). $^{13}$C NMR (CDCl$_3$, 400 MHz): δ 181.0, 154.8, 153.4, 148.6, 133.1, 132.6, 130.1, 124.2, 32.1, 29.5, 26.8, 24.7, 24.3, 20.2. ESI [M + H] = 367.4.

*Benzyl-2-(3,5-dichloropyridin-4-yl)hydrazinecarboxylate (34).* Following the general procedure using the **8** and benzyl chloroformate, **34** was obtained as a yellow oil (26.6 mg, 71%). $^1$H NMR (CDCl$_3$, 400 MHz): δ 8.29 (2H, s), 7.71 (1H, s, N−H), 7.36−7.21 (5H, m), 6.80 (1H, s, N−H), 3.58 (2H, s). $^{13}$C NMR (CDCl$_3$, 400 MHz): δ 158.7, 155.0, 150.4, 139.4, 133.4, 133.1, 131.5, 121.9, 69.1. ESI [M + H] = 312.9. Purity: 88%.

*N-Benzyl-2-(3,5-dichloropyridin-4-yl)hydrazinecarboxamide (35).* 3,5-Dichloro-4-hydrazinylpyridine (**8**, 40.0 mg, 0.2 mmol) was dissolved in dichloromethane (20 mL), and then carbonyl diimidazole (36.4 mg, 0.4 mmol) and triethylamine (40.0 μL, 0.4 mmol) were added. The reaction mixture was stirred at room temperature for 1 h. The white precipitate was filtered, washed with dichloromethane, and dried under reduced pressure to give *N′*-(3,5-dichloropyridin-4-yl)-1*H*-imidazole-1-carbohydrazide (46.5 mg, 76%) The compound was dissolved in dimethylformaimide (2.0 mL), and then benzyl amine (36.5 μL, 0.3 mmol) and triethylamine (35.0 μL, 0.4 mmol) were added. The reaction mixture was stirred at room temperature for 2 h. Then the dimethylformamide was removed by rotary evaporator. The residue was taken up in water and extracted with ethyl acetate (2×). The combined organic layer was dried over sodium sulfate, filtered, and evaporated. The residue was purified by silica gel column chromatography (CH$_3$Cl:methanol = 20:1) to give **35** as a white solid (34.5 mg, 65%); mp 215−217 °C. $^1$H NMR (CDCl$_3$, 400 MHz): δ 8.18 (2H, s), 7.39 (1H, s, N−H), 7.28−7.18 (5H, m), 6.97 (1H, s, N−H), 6.10 (1H, t, J = 5.0 Hz, N−H), 4.37 (2H, d, J = 4.8 Hz). $^{13}$C NMR (CDCl$_3$, 400 MHz): δ 166.2, 154.7, 152.9, 144.2, 133.2, 132.1, 132.0, 123.4, 40.8. ESI [M + H] = 312.9.

*N′-(3,5-Dichloropyridin-4-yl)cinnamohydrazide (36).* Following the general procedure using the **8** and *trans*-cinnamoic acid, **36** was obtained as a white solid (23.7 mg, 78%); mp 184−186 °C. $^1$H NMR

(CDCl$_3$, 400 MHz): δ 8.33 (2H, s), 7.71 (1H, d, J = 16.0 Hz), 7.68 (1H, d, J = 4.0 Hz, N−H), 7.53−7.38 (5H, m), 7.01 (1H, d, J = 4.0 Hz, N−H), 6.42 (1H, d, J = 15.6 Hz). $^{13}$C NMR (CDCl$_3$, 400 MHz): δ 172.4, 152.2, 151.6, 147.2, 137.5, 133.0, 131.5, 130.5, 121.6, 118.2. ESI [M + H] = 309.0. Purity: 94%.

*(±)-N′-(3,5-Dichloropyridin-4-yl)-1,2,3,4-tetrahydronaphthalene-2-carbohydrazide (37).* Following the general procedure using the **8** and (±)-1,2,3,4-tetrahydronaphthalene-2-carboxylic acid, **37** was obtained as a white solid (25.1 mg, 79%); mp 219−211 °C. $^1$H NMR (CDCl$_3$, 400 MHz): δ 9.15 (2H, s), 8.48 (1H, d, J = 4.8 Hz, N−H), 7.67−7.56 (4H, m), 7.36 (1H, d, J = 4.8 Hz, N−H), 3.05−2.84 (4H, m), 2.64−2.61 (1H, m), 2.14−1.87 (2H, m). $^{13}$C NMR (CDCl$_3$, 400 MHz): δ 181.2, 152.9, 151.4, 138.6, 137.5, 131.8, 131.7, 128.7, 128.5, 122.5, 34.3, 25.7, 21.9, 19.6. ESI [M + H] = 337.9.

*N′-(3,5-Dichloropyridin-4-yl)-2,3-dihydro-1H-indene-2-carbohydrazide (38).* Following the general procedure using the **8** and Indane-2-carboxylic acid, **38** was obtained as a white solid (19.8 mg, 70%); mp 237−239 °C. $^1$H NMR (DMSO-$d_6$, 400 MHz): δ 8.31 (2H, s), 7.68 (1H, d, J = 3.2 Hz, N−H), 7.22−7.16 (4H, m), 6.86 (1H, d, J = 4.0 Hz, N−H), 3.26−3.18 (5H, m). $^{13}$C NMR (DMSO-$d_6$, 400 MHz): δ 181.5, 152.5, 151.6, 145.1, 129.2, 126.5, 121.7, 38.0, 30.6. ESI [M + H] = 323.9. Purity: 92%.

*(±)-N′-(3,5-Dichloropyridin-4-yl)-1,2-dihydrocyclobutabenzene-1-carbohydrazide (39).* Following the general procedure using the **8** and (±)-benzocyclobutanoic acid, **39** was obtained as a white solid (18.3 mg, 67%); mp 237−239 °C. $^1$H NMR (CDCl$_3$, 400 MHz): δ 8.31 (2H, s), 8.01 (1H, d, J = 4.0 Hz, N−H), 7.32−7.30 (2H, m), 7.22 (1H, t, J = 4.0 Hz), 7.17 (1H, d, J = 4.0 Hz), 6.85 (1H, d, J = 4.0 Hz, N−H). 4.30−4.28 (1H, m), 3.60 (1H, dd, J = 14.0, 6.4 Hz), 3.397 (1H, dd, J = 14.2, 2.4 Hz). $^{13}$C NMR (CDCl$_3$, 400 MHz): δ 178.6, 166.5, 155.9, 154.2, 141.0, 136.4, 135.7, 129.4, 129.4, 122.5, 40.0, 32.0. ESI [M + H] = 309.3. Purity: 94%.

*N′-(3,5-Dichloropyridin-4-yl)-1H-indole-2-carbohydrazide (40).* Following the general procedure using the **8** and 2-indolic acid, **40** was obtained as a brown solid (29.3 mg, 94%); mp 273−275 °C. $^1$H NMR (DMSO-$d_6$, 400 MHz): δ 11.65 (1H, s, N−H$_{indole}$), 10.77 (1H, s), 8.52 (1H, s, N−H), 8.24 (2H, s), 7.62 (1H, d, J = 8.4 Hz), 7.40 (1H, d, J = 8.4 Hz), 7.22 (1H, s, N−H), 7.17(1H, t, J = 7.8 Hz), 7.03 (1H, t, J = 7.6 Hz). $^{13}$C NMR (DMSO-$d_6$, 400 MHz): δ 166.8, 153.2, 151.6, 140.6, 132.2, 130.0, 126.5, 124.3, 122.3, 119.0, 114.1, 104.5. ESI [M + H] = 322.6. Purity: 94%.

*N′-(3,5-Dichloropyridin-4-yl)-2-(naphthalen-1-yl)acetohydrazide (41).* Following the general procedure using the **8** and naphthalen-1-acetic acid, **41** was obtained as a white solid (28.4 mg, 71%); mp 221−223 °C. $^1$H NMR (CDCl$_3$, 400 MHz): δ 8.47 (1H, s, N−H), 8.11 (2H, s), 7.91−7.76 (3H, m), 7.49−7.37 (4H, m), 6.84 (1H, s, N−H), 3.99 (2H, s). $^{13}$C NMR (CDCl$_3$, 400 MHz): δ 179.3, 154.5, 153.5, 139.2, 137.1, 133.6, 133.4, 133.3, 133.1, 130.7, 130.1, 128.0, 123.9, 112.9, 38.1. ESI [M + H] = 347.5.

*N′-(3,5-Dichloropyridin-4-yl)-2-(naphthalen-2-yl)acetohydrazide (42).* Following the general procedure using the **8** and naphthalen-2-acetic acid, **42** was obtained as a white solid (31.6 mg, 81%); mp 240−242 °C. $^1$H NMR (CDCl$_3$, 400 MHz): δ 10.47 (1H, s, N−H), 8.24 (2H, s), 7.86−7.81 (4H, m), 7.47−7.40 (2H + N − H, m), 3.64 (2H, s). $^{13}$C NMR (CDCl$_3$, 400 MHz): δ 176.1, 153.1, 151.5, 136.5, 136.4, 135.2, 131.0, 130.8, 130.6, 130.5, 130.4, 129.1, 128.5, 119.3, 35.6. ESI [M + H] = 347.6. Purity: 90%.

*N′-(3,5-Dichloropyridin-4-yl)-3-(naphthalen-1-yl)propanehydrazide (43).* Following the general procedure using the **8** and naphthalen-1-propionic acid, **43** was obtained as a white solid (36.3 mg, 90%); mp 206−208 °C. $^1$H NMR (CDCl$_3$, 400 MHz): δ 8.39 (1H, s, N−H), 8.21 (2H, s), 7.99−7.96 (1H, m), 7.85−7.83 (1H, m), 7.71 (1H, d, J = 8.4 Hz), 7.48−7.45 (2H, m), 7.34 (1H, t, J = 7.6 Hz), 7.27 (1H, d, J = 6.8 Hz), 6.82 (1H, s, N−H), 3.39 (2H, t, J = 7.8 Hz), 2.62 (2H, t, J = 7.6 Hz). $^{13}$C NMR (CDCl$_3$, 400 MHz): δ 178.4, 152.6, 139.6, 137.1, 134.4, 131.6, 129.9, 128.6, 128.3, 128.1, 128.0, 126.9, 125.4, 122.0, 28.6, 23.4. ESI [M + H] = 361.1.

*3-Cyclopentyl-N′-(3,5-dichloropyridin-4-yl)propanehydrazide (44).* Following the general procedure using the **8** and cyclopentylpropionic acid, **44** was obtained as a white solid (23.0 mg, 93%); mp 181−183 °C. $^1$H NMR (CDCl$_3$, 400 MHz): δ 8.29 (2H, s),

7.69 (1H, d, $J$ = 3.6 Hz, N–H), 6.83 (1H, d, $J$ = 3.6 Hz, N–H), 2.23 (2H, t, $J$ = 7.6 Hz), 1.76–1.48 (11H, m). $^{13}$C NMR (CDCl$_3$, 400 MHz): $\delta$ 181.1, 154.8, 153.4, 124.2, 36.1, 28.9, 28.4, 27.0, 20.4. ESI [M + H] = 303.6.

*3-Cyclohexyl-N′-(3,5-dichloropyridin-4-yl)propanehydrazide (45).* Following the general procedure using the **8** and cyclohexylpropionic acid, **45** was obtained as a white solid (23.7 mg, 90%); mp 198–200 °C. $^1$H NMR (CDCl$_3$, 400 MHz): $\delta$ 8.30 (2H, s), 7.55 (1H, d, $J$ = 3.6 Hz, N–H), 6.84 (1H, d, $J$ = 3.6 Hz, N–H), 2.23 (2H, t, $J$ = 7.8 Hz), 1.68–1.62 (5H, m), 1.52 (2H, q, $J$ = 7.6 Hz), 1.23–1.12 (4H, m), 0.90–0.81 (2H, m). $^{13}$C NMR (CDCl$_3$, 400 MHz): $\delta$ 172.5, 148.3, 147.0, 122.8, 37.1, 32.9, 32.3, 31.0, 26.4, 26.1. ESI [M + H] = 318.0.

*2-Cyclohexyl-N′-(3,5-dichloropyridin-4-yl)acetohydrazide (46).* Following the general procedure using the **8** and cycloheptylacetic acid, **46** was obtained as a white solid (18.1 mg, 78%); mp 193–195 °C. $^1$H NMR (CDCl$_3$, 400 MHz): $\delta$ 8.30 (2H, s), 7.60 (1H, s, N–H), 6.85 (1H, d, $J$ = 2.8 Hz, N–H), 2.08 (2H, d, $J$ = 6.8 Hz), 1.83–1.61 (5H, m), 1.28–1.00 (4H, m), 0.98–0.88 (2H, m). $^{13}$C NMR (CDCl$_3$, 400 MHz): $\delta$ 180.4, 155.0, 153.6, 124.6, 38.4, 31.2, 29.3, 21.6, 21.4. ESI [M + H] = 303.8.

*2-Cycloheptyl-N′-(3,5-dichloropyridin-4-yl)acetohydrazide (47).* Following the general procedure using the **8** and cyclohexylacetic acid, **47** was obtained as a white solid (18.2 mg, 79%); mp 181–183 °C. $^1$H NMR (CDCl$_3$, 400 MHz): $\delta$ 8.29 (2H, s), 7.59 (1H, d, $J$ = 3.6 Hz, N–H), 6.85 (1H, d, $J$ = 3.6 Hz, N–H), 2.21–1.89 (6H, m), 1.54–1.47 (3H, m), 1.28–1.05 (6H, m). $^{13}$C NMR (CDCl$_3$, 400 MHz): $\delta$ 189.6, 160.6, 158.9, 125.6, 26.5, 25.9, 23.0, 21.0, 19.1. ESI [M + H] = 317.5.

*4-Cyclohexyl-N′-(3,5-dichloropyridin-4-yl)butanehydrazide (48).* Following the general procedure using the **8** and cyclohexylbutanoic acid, **48** was obtained as a white solid (17.9 mg, 77%); mp 159–161 °C. $^1$H NMR (CDCl$_3$, 400 MHz): $\delta$ 8.29 (2H, s), 7.58 (1H, d, $J$ = 3.2 Hz, N–H), 6.83 (1H, d, $J$ = 4.0 Hz, N–H), 2.19 (2H, t, $J$ = 7.6 Hz), 1.81–1.55 (9H, m), 1.32–1.07 (4H, m), 0.98–0.78 (2H, m). $^{13}$C NMR (CDCl$_3$, 400 MHz): $\delta$ 179.1, 152.9, 151.5, 122.4, 31.9, 31.4, 28.1, 27.3, 20.1, 19.8, 15.5. ESI [M + H] = 312.9.

*N′-(3,5-Dichloropyridin-4-yl)-2-adamantylacetohydrazide (49).* Following the general procedure using the **8** and 2-adamantanylacetic acid, **49** was obtained as a white solid (30.7 mg, 90%); mp 195–197 °C. $^1$H NMR (CDCl$_3$, 400 MHz): $\delta$ 8.29 (2H, s), 7.52 (1H, d, $J$ = 4.0 Hz, N–H), 6.90 (1H, d, $J$ = 4.0 Hz, N–H), 1.90–1.86 (5H, m), 1.69–1.59 (12H, m). $^{13}$C NMR (CDCl$_3$, 400 MHz): $\delta$ 176.8, 152.8, 151.5, 122.5, 43.6, 37.3, 30.9, 27.0, 22.1. ESI [M + H] = 355.9.

*N′-(3,5-Dichloropyridin-4-yl)-2-adamantyhydrazide (50).* Following the general procedure using the **8** and 2-adamantanylcarboxylic acid, **50** was obtained as a white solid (27.6 mg, 90%); mp 207–209 °C. $^1$H NMR (CDCl$_3$, 400 MHz): $\delta$ 8.30 (2H, s), 7.82 (1H, d, $J$ = 4.0 Hz, N–H), 6.83 (1H, d, $J$ = 4.0 Hz, N–H), 2.05–2.01 (3H, m), 1.93–1.88 (6H, m), 1.77–1.68 (6H, m). $^{13}$C NMR (CDCl$_3$, 400 MHz): $\delta$ 183.5, 152.8, 151.9, 122.6, 35.2, 33.4, 30.8, 30.6, 21.4. ESI [M + H] = 341.9.

*N′-(3,5-Dichloropyridin-4-yl)-3-bromoadamantylhydrazide (51).* Following the general procedure using the **8** and 3-bromoadamantylcarboxylic acid, **51** was obtained as a white solid (28.3 mg, 79%); mp 214–216 °C. $^1$H NMR (CDCl$_3$, 400 MHz): $\delta$ 8.31 (2H, s), 7.78 (1H, d, $J$ = 4.0 Hz, N–H), 6.79 (1H, d, $J$ = 4.0 Hz, N–H), 2.46 (2H, s), 2.36–2.24 (6H, m), 1.73–1.55 (6H, m). $^{13}$C NMR (CDCl$_3$, 400 MHz): $\delta$ 183.7, 155.7, 154.3, 125.4, 61.9, 47.9, 46.0, 34.3, 31.2, 28.2. ESI [M + H] = 419.9.

*N′-(3,5-Dichloropyridin-4-yl)-3,5-dimethyladamantylhydrazide (52).* Following the general procedure using the **8** and 3,5-dimethyladamantylcarboxylic acid, **52** was obtained as a white solid (31.6 mg 93%); mp 162–164 °C. $^1$H NMR (CDCl$_3$, 400 MHz): $\delta$ 8.29 (2H, s), 7.82 (1H, d, $J$ = 4.0 Hz, N–H), 6.79 (1H, d, $J$ = 4.4 Hz, N–H), 2.14–2.13 (1H, m), 1.71 (2H, d, $J$ = 2.8 Hz), 1.51 (4H, q, $J$ = 12.6 Hz), 1.51 (4H, q, $J$ = 10.6 Hz), 1.36–1.15 (2H, m), 0.85 (6H, s). $^{13}$C NMR (CDCl$_3$, 400 MHz): $\delta$ 183.3, 152.8, 151.8, 122.7, 46.1, 40.1, 37.5, 37.2, 32.0, 24.8, 24.1, 22.7. ESI [M + H] = 369.8.

*N′-(3,5-Dichloropyridin-4-yl)-1-noradamantylhydrazide (53).* Following the general procedure using the **8** and 1-noradamantylcar-

boxylic acid, **53** was obtained as a white solid (24.0 mg, 71%); mp 198–200 °C. $^1$H NMR (CDCl$_3$, 400 MHz): $\delta$ 8.30 (2H, s), 7.74 (1H, d, $J$ = 4.0 Hz, N–H), 6.85 (1H, d, $J$ = 3.6 Hz, N–H), 2.70 (1H, t, $J$ = 6.6 Hz), 2.33 (2H, s), 2.01–1.99 (2H, m), 1.48–1.66 (4H, m), 1.64–1.59 (4H, m). $^{13}$C NMR (CDCl$_3$, 400 MHz): $\delta$ 185.1, 154.6, 153.6, 124.4, 51.5, 44.2, 43.8, 41.1, 40.5, 33.7, 33.6, 30.6. ESI [M + H] = 328.0. Purity: 92%.

*N′-(3,5-Dichloropyridin-4-yl)bicyclo[2.2.1]heptane-2-carbohydrazide (54).* Following the general procedure using the **8** and 2-norbornylcarboxylic acid, **54** was obtained as a white solid (26.1 mg, 84%); mp 180–182 °C. $^1$H NMR (CDCl$_3$, 400 MHz): $\delta$ 8.31 (2H, s), 7.60 (1H, d, $J$ = 3.6 Hz, N–H), 6.84 (1H, d, $J$ = 4.0 Hz, N–H), 2.68–2.64 (1H, m), 2.48–2.26 (3H, m), 1.65–1.27 (7H, m). $^{13}$C NMR (CDCl$_3$, 400 MHz): $\delta$ 182.5, 154.8, 153.6, 124.5, 41.9, 37.7, 37.3, 33.3, 27.1, 24.8, 19.6. ESI [M + H] = 301.7.

*2-(Bicyclo[2.2.1]heptan-2-yl)-N′-(3,5-dichloropyridin-4-yl)-acetohydrazide (55).* Following the general procedure using the **8** and 2-norbornylacetic acid, **55** was obtained as a white solid (29.9 mg, 80%); mp 173–175 °C. $^1$H NMR (CDCl$_3$, 400 MHz): $\delta$ 8.30 (2H, s), 7.55 (1H, d, $J$ = 3.6 Hz, N–H), 6.86 (1H, d, $J$ = 4.0 Hz, N–H), 2.13 (2H, d, $J$ = 7.6 Hz), 2.04–1.99 (1H, m), 1.72–1.40 (8H, m), 1.24–1.09 (2H, m). $^{13}$C NMR (CDCl$_3$, 400 MHz): $\delta$ 179.5, 154.8, 149.6, 127.4, 52.6, 48.6, 39.4, 28.7, 27.4, 19.5, 18.4. ESI [M + H] = 315.7.

*N′-(3,5-Dichloropyridin-4-yl)bicyclo[2.2.1]hept-5-ene-2-carbohydrazide (56).* Following the general procedure using the **8** and 5-norbornenyl-2-carboxylic acid, **56** was obtained as a white solid (20.1 mg, 69%); mp 186–188 °C. $^1$H NMR (CDCl$_3$, 400 MHz): $\delta$ 8.29 (2H, s), 7.57 (1H, d, $J$ = 4.0 Hz, N–H), 6.80 (1H, d, $J$ = 4.0 Hz, N–H), 6.22 (1H, q, $J$ = 3.0 Hz), 5.93 (1H, q, $J$ = 3.0 Hz), 3.18 (1H, s), 2.94–2.88 (2H, m), 1.98–1.91 (1H, m), 1.58–1.24 (3H, m). $^{13}$C NMR (CDCl$_3$, 400 MHz): $\delta$ 181.9, 154.5, 153.3, 143.4, 136.5, 124.2, 49.5, 47.2, 43.0, 39.2, 24.8. ESI [M + H] = 299.7.

**Biological Methods.** *Measurement of Ethidium Bromide Accumulation in hP2X$_7$-Expressing HEK 293 Cells.* hP2X$_7$-expressing HEK 293 cells were resuspended at 2.5 × 10$^6$ cells/mL in assay buffer composed of 10 mM HEPES, 5 mM $N$-methyl-D-glutamine, 5.6 mM KCl, 10 mM D-glucose, and 0.5 mM CaCl$_2$ (pH 7.4) supplemented with either 280 mM sucrose or 140 mM NaCl, and an 80 $\mu$L aliquot was added to each well of a 96-well plates. To each was added test compounds or 1-[$N$,$O$-bis(1,5-isoquinolinesulfonyl)-$N$-methyl-L-tyrosyl]-4-phenylpiperazine (**1**) as the positive control, followed by the hP2X$_7$R agonist benzoylbenzoyl ATP (BzATP). The plates were incubated at 37 °C for 2 h, and the cellular accumulation of ethidium ion was determined by measuring fluorescence with a Bio-Tek FL600 fluorescent plate reader (excitation wavelength 530 nm; emission wavelength 590 nm). The IC$_{50}$ value of each compound was measured and compared with that of **9**.

*Enzyme-Linked Immunosorbent Assay (ELISA) of Human IL-1β in Differentiated THP-1 Cells.* Human monocytic leukemia THP-1 cells were plated at 2 × 10$^5$ cells/well of 96-well plates. To differentiate THP-1 cells into macrophages, the cells were incubated with 25 ng/mL LPS and 10 ng/mL IFN-γ for 3 h. The differentiated cells were incubated at 37 °C with KN-62 (**1**) or test compounds for 30 min, followed by 1 mM BzATP for an additional 30 min. The culture supernatants were collected by centrifugation at ∼250$g$ for 5 min and stored as aliquots at −70 °C. IL-1β concentrations were measured by ELISA, using antihuman IL-1β antibody as the capture antibody and a biotinylated antihuman IL-1β antibody for detection (eBioscience). The concentration of IL-1β in each sample was compared with that of a standard curve of recombinant human IL-1β, with the basal level of IL-1β subtracted from all measurements.

*Measurement of iNOS and COX-2 Expression by Western Blotting.* Treated cells were collected, washed with cold phosphate-buffered saline (PBS), lysed on ice for 30 min in 100 $\mu$L lysis buffer [120 mM NaCl, 40 mM Tris (pH 8), 0.1% NP40 (Nonidet P-40)], and centrifuged at ∼10000$g$ for 30 min at 4 °C. The supernatants were withdrawn and their protein concentrations were determined using a BCA protein assay kit (Pierce, Rockford, IL). Aliquots of the lysates, containing 30 $\mu$g of protein, were boiled for 5 min and electrophoresed

on 10% SDS-polyacrylamide gels. The proteins were transferred onto nitrocellulose membranes, which were incubated with primary antibodies against iNOS or COX-2 or mouse monoclonal anti-$\beta$-actin antibodies, followed by incubation with secondary antimouse or antirabbit antibodies. Protein bands were detected using an enhanced chemiluminescence Western blotting detection kit (Pierce Biotechnology, Rockford, IL).

*Measurement of Nitrite Production in Differentiated THP-1 Cells.* THP-1 ($2 \times 105$ cells/mL) prepared as above were cultured in 48-well plates for 24 h, and nitrite concentrations in the culture media were measured by incubating each with Griess reagent (1% sulfanilamide, 0.1% $N$-1-naphthylethylenediamine dihydrochloride, and 2.5% phosphoric acid) for 10 min and measuring absorbance at 540 nm.

## ■ ASSOCIATED CONTENT

### Ⓢ Supporting Information

Analytical data of element analysis of final compounds for purity. This material is available free of charge via the Internet at http://pubs.acs.org.

## ■ AUTHOR INFORMATION

### Corresponding Author

*Phone: +82-62-715-2502. Fax: +82-62-715-2484. E-mail: yongchul@gist.ac.kr.

### Notes

The authors declare no competing financial interest.

## ■ ACKNOWLEDGMENTS

## ■ ABBREVIATIONS USED

ATP, adenosine 5′-triphosphate; HEPES, 4-(2-hydroxyethyl)-1-piperazineethanesulfonic acid; BCA, bicinchoninic acid; ELISA, enzyme-linked immunosorbent assay; SDS, sodium dodecyl sulfate; $IC_{50}$, half-maximal inhibitory concentration; IL, interleukin; LPS, lipopolysaccharide; IFN, interferon; COX, cyclooxygenase; NOS, nitric oxide synthase; AP-1, activator protein 1; ESI, electrospray ionization; NMR, nuclear magnetic resonance

## ■ REFERENCES

(1) Wang, X. H.; Arcuino, G.; Takano, T.; Lin, J.; Peng, W. G.; Wan, P. L.; Li, P. J.; Xu, Q. W.; Liu, Q. S.; Goldman, S. A.; Nedergaard, M. P2X$_7$ receptor inhibition improves recovery after spinal cord injury. *Nature Med.* **2004**, *10* (8), 821−827.

(2) Clark, A. K.; Staniland, A. A.; Marchand, F.; Kaan, T. K. Y.; McMahon, S. B.; Malcangio, M. P2X7-dependent release of interleukin-1$\beta$ and nociception in the spinal cord following lipopolysaccharide. *J. Neurosci.* **2009**, *30* (2), 573−582.

(3) Honore, P.; Donnelly-Roberts, D.; Namovic, M.; Zhong, C.; Wade, C.; Chandran, P.; Zhu, C.; Carroll, W.; Perez-Medrano, A.; Iwakura, Y.; Jarvis, M. F. The antihyperalgesic activity of a selective P2X$_7$ receptor antagonist, A-839977, is lost in IL-1$\alpha\beta$ knockout mice. *Behav. Brain Res.* **2009**, *204* (1), 77−81.

(4) Jarvis, M. F. The neural−glial purinergic receptor ensemble in chronic pain states. *Trends Neurosci.* **2009**, *33* (1), 48−57.

(5) Gudipaty, L.; Humphreys, B. D.; Buell, G.; Dubyak, G. R. Function and expression of the human P2X$_7$ nucleotide receptor in peripheral blood leukocytes. *FASEB J.* **2000**, *14* (4), A183−A183.

(6) Narcisse, L.; Scemes, E.; Zhao, Y. M.; Lee, S. C.; Brosnan, C. F. The cytokine IL-1 beta transiently enhances P2X($_7$) receptor expression and function in human astrocytes. *Glia* **2005**, *49* (2), 245−258.

(7) Lappin, S.; Gunthorpe, M. Characterisation of native P2X$_7$ receptors expressed on non-neuronal cells from cultures of rat dorsal root ganglia. *Neuron Glia Biol.* **2007**, *2*, S174−S174.

(8) Sengstake, S.; Boneberg, E. M.; Illges, H. CD21 and CD62L shedding are both inducible via P2X$_7$Rs. *Int. Immunol.* **2006**, *18* (7), 1171−1178.

(9) Brändle, U.; Kohler, K.; Wheeler-Schilling, T. H. Expression of the P2X$_7$-receptor subunit in neurons of the rat retina. *Mol. Brain Res.* **1998**, *62* (1), 106−109.

(10) Vayro, S.; Hamilton, N.; Kirchhoff, F.; Gorecki, D.; Butt, A. P2X$_7$ knock-out mice exhibit decreased ATP and glutamate mediated calcium signaling in white matter astrocytes: implications for astroglial communication. *Neuron Glia Biol.* **2007**, *2*, S173−S173.

(11) Liu, Y. P.; Yang, C. S.; Chen, M. C.; Sun, S. H.; Tzeng, S. F. Ca$^{2+}$-dependent reduction of glutamate aspartate transporter GLAST expression in astrocytes by P2X$_7$ receptor-mediated phosphoinositide 3-kinase signaling. *J. Neurochem.* **2010**, *113* (1), 213−227.

(12) Verhoef, P. A.; Kertesy, S. B.; Lundberg, K.; Kahlenberg, J. M.; Dubyak, G. R. Inhibitory effects of chloride on the activation of caspase-1, IL-1 beta secretion, and cytolysis by the P2X$_7$ receptor. *J. Immunol.* **2005**, *175* (11), 7623−7634.

(13) Verhoef, P. A.; Estacion, M.; Schilling, W.; Dubyak, G. R. P2X$_7$ receptor-dependent blebbing and the activation of Rho-effector kinases, caspases, and IL-1 beta release. *J. Immunol.* **2003**, *170* (11), 5728−5738.

(14) Eslick, G. D.; Thampan, B. V.; Nalos, M.; McLean, A. S.; Sluyter, R. Circulating interleukin-18 concentrations and a loss-of-function P2X$_7$ polymorphism in heart failure. *Int. J. Cardiol.* **2009**, *137* (1), 81−83.

(15) Smart, M. L.; Gu, B.; Panchal, R. G.; Wiley, J.; Cromer, B.; Williams, D. A.; Petrou, S. P2X$_7$ receptor cell surface expression and cytolytic pore formation are regulated by a distal C-terminal region. *J. Biol. Chem.* **2003**, *278* (10), 8853−8860.

(16) Brough, D.; Rothwell, N. J. Caspase-1-dependent processing of pro-interlukin-1$\beta$ is cytosolic and precedes cell death. *J. Cell Sci.* **2007**, *120* (5), 772−781.

(17) Clark, A. K.; Wodarski, R.; Guida, F.; Sasso, O.; Malcangio, M. Cathepsin S release from primary cultured microglia is regulated by the P2X$_7$ receptor. *Glia* **2010**, *58* (14), 1710−1726.

(18) Labasi, J. M.; Petrushova, N.; Donovan, C.; McCurdy, S.; Lira, P.; Payette, M. M.; Brissette, W.; Wicks, J. R.; Audoly, L.; Gabel, C. A. Absence of the P2X$_7$ receptor alters leukocyte function and attenuates an inflammatory response. *J. Immunol.* **2002**, *168* (12), 6436−6445.

(19) Iavicoli, I.; Marinaccio, A.; Castellino, N.; Carelli, G. Altered cytokine production in mice exposed to lead acetate. *Int. J. Immunopathol. Pharmacol.* **2004**, *17* (2 Suppl), 97.

(20) Basso, A. M.; Bratcher, N. A.; Harris, R. R.; Jarvis, M. F.; Decker, M. W.; Rueter, L. E. Behavioral profile of P2X$_7$ receptor knockout mice in animal models of depression and anxiety: Relevance for neuropsychiatric disorders. *Behav. Brain Res.* **2009**, *198* (1), 83−90.

(21) Taylor, S. R. J.; Gonzalez-Begne, M.; Sojka, D. K.; Richardson, J. C.; Sheardown, S. A.; Harrison, S. M.; Pusey, C. D.; Tam, F. W. K.; Elliott, J. I. Lymphocytes from P2X$_7$-deficient mice exhibit enhanced P2X$_7$ responses. *J. Leukocyte Biol.* **2009**, *85* (6), 978−986.

(22) Carroll, W. A.; Donnelly-Roberts, D.; Jarvis, M. F. Selective P2X$_7$ receptor antagonists for chronic inflammation and pain. *Purinergic Signalling* **2009**, *5* (1), 63−73.

(23) Takenouchi, T.; Sekiyama, K.; Sekigawa, A.; Fujita, M.; Waragai, M.; Sugama, S.; Iwamaru, Y.; Kitani, H.; Hashimoto, M. P2X$_7$ Receptor Signaling Pathway as a Therapeutic Target for Neurodegenerative Diseases. *Arch. Immunol. Ther. Exp.* **2010**, *58*, 91−96.

(24) Skaper, S. D.; Debetto, P.; Giusti, P. The P2X$_7$ purinergic receptor: From physiology to neurological disorders. *FASEB J.* **2010**, *24* (2), 337−345.

(25) Wang, L. Y.; Cai, W. Q.; Chen, P. H.; Deng, Q. Y.; Zhao, C. M. Downregulation of P2X₇ receptor expression in rat oligodendrocyte precursor cells after hypoxia ischemia. *Glia* **2009**, *57* (3), 307–319.

(26) Milius, D.; Sperlagh, B.; Illes, P. Up-regulation of P2X₇ receptor-immunoreactivity by in vitro ischemia on the plasma membrane of cultured rat cortical neurons. *Neurosci. Lett.* **2008**, *446* (1), 45–50.

(27) Tsuda, M.; Tozaki-Saitoh, H.; Inoue, K. Pain and purinergic signaling. *Brain Res. Rev.* **2009**, *63* (1–2), 222–232.

(28) Burnstock, G. Purinergic receptors and pain. *Curr. Pharm. Des.* **2009**, *15* (15), 1717–1735.

(29) Lee, J. Y.; Yu, J.; Cho, W. J.; Ko, H.; Kim, Y. C. Synthesis and structure–activity relationships of pyrazolodiazepine derivatives as human P2X₇ receptor antagonists. *Bioorg. Med. Chem. Lett.* **2009**, *19* (21), 6053–6058.

(30) Chen, X.; Pierce, B.; Naing, W.; Grapperhaus, M. L.; Phillion, D. P. Discovery of 2-chloro-*N*-((4,4-difluoro-1-hydroxycyclohexyl)-methyl)-5-(5-fluoropyrimidin-2-yl)benzamide as a potent and CNS penetrable P2X₇ receptor antagonist. *Bioorg. Med. Chem. Lett.* **2010**, *20* (10), 3107–3111.

(31) Chambers, L. J.; Stevens, A. J.; Moses, A. P.; Michel, A. D.; Walter, D. S.; Davies, D. J.; Livermore, D. G.; Fonfria, E.; Demont, E. H.; Vimal, M.; Theobald, P. J.; Beswick, P. J.; Gleave, R. J.; Roman, S. A.; Senger, S. Synthesis and structure–activity relationships of a series of (1*H*-pyrazol-4-yl)acetamide antagonists of the P2X₇ receptor. *Bioorg. Med. Chem. Lett.* **2009**, *20* (10), 3161–3164.

(32) Friedle, S. A.; Curet, M. A.; Watters, J. J. Recent patents on novel P2X(₇) receptor antagonists and their potential for reducing central nervous system inflammation. *Recent Pat. CNS Drug Discovery* **2009**, *5* (1), 35–45.

(33) Baraldi, P. G.; Nuñez, M. D. C.; Morelli, A.; Falzoni, S.; Di Virgilio, F.; Romagnoli, R. Synthesis and biological activity of *N*-arylpiperazine-modified analogues of KN-62, a potent antagonist of the purinergic P2X₇ receptor. *J. Med. Chem.* **2003**, *46* (8), 1318–1329.

(34) Humphreys, B. D.; Virginio, C.; Surprenant, A.; Rice, J.; Dubyak, G. R. Isoquinolines as antagonists of the P2X₇ nucleotide receptor: High selectivity for the human versus rat receptor homologues. *Mol. Pharmacol.* **1998**, *54* (1), 22–32.

(35) Hidaka, H.; Okazaki, K. KN-62: A specific Ca²⁺/calmodulin-dependent protein kinase inhibitor as a putative function-searching probe for intracellular signal transduction. *Cardiovasc. Drug Rev.* **1996**, *14* (1), 84.

(36) Furber, M.; Alcaraz, L.; Bent, J. E.; Beyerbach, A.; Bowers, K.; Braddock, M.; Caffrey, M. V.; Cladingboel, D.; Collington, J.; Donald, D. K.; Fagura, M.; Ince, F.; Kinchin, E. C.; Laurent, C.; Lawson, M.; Luker, T. J.; Mortimore, M. M. P.; Pimm, A. D.; Riley, R. J.; Roberts, N.; Robertson, M.; Theaker, J.; Thorne, P. V.; Weaver, R.; Webborn, P.; Willis, P. Discovery of potent and selective adamantane-based small-molecule P2X₇ receptor antagonists/interleukin-1β inhibitors. *J. Med. Chem.* **2007**, *50* (24), 5882–5885.

(37) Baxter, A.; Bent, J.; Bowers, K.; Braddock, M.; Brough, S.; Fagura, M.; Lawson, M.; McInally, T.; Mortimore, M.; Robertson, M.; Weaver, R.; Webborn, P. Hit-to-lead studies: The discovery of potent adamantane amide P2X₇ receptor antagonists. *Bioorg. Med. Chem. Lett.* **2003**, *13* (22), 4047–4050.

(38) Nelson, D. W.; Sarris, K.; Kalvin, D. M.; Namovic, M. T.; Grayson, G.; Donnelly-Roberts, D. L.; Harris, R.; Honore, P.; Jarvis, M. F.; Faltynek, C. R.; Carroll, W. A. Structure–activity relationship studies on *N*-aryl carbohydrazide P2X₇ antagonists. *J. Med. Chem.* **2008**, *51* (10), 3030–3034.

(39) Florjancic, A. S.; Peddi, S.; Perez-Medrano, A.; Li, B.; Namovic, M. T.; Grayson, G.; Donnelly-Roberts, D. L.; Jarvis, M. F.; Carroll, W. A. Synthesis and in vitro activity of 1-(2,3-dichlorophenyl)-*N*-(pyridin-3-ylmethyl)-1*H*-1,2,4-triazol-5-amine and 4-(2,3-dichlorophenyl)-*N*-(pyridin-3-ylmethyl)-4*H*-1,2,4-triazol-3-amine P2X₇ antagonists. *Bioorg. Med. Chem. Lett.* **2008**, *18* (6), 2089–2092.

(40) Perez-Medrano, A.; Donnelly-Roberts, D. L.; Honore, P.; Hsieh, G. C.; Namovic, M. T.; Peddi, S.; Shuai, Q.; Wang, Y.; Faltynek, C. R.; Jarvis, M. F.; Carroll, W. A. Discovery and biological evaluation of novel cyanoguanidine P2X₇ antagonists with analgesic activity in a rat model of neuropathic pain. *J. Med. Chem.* **2009**, *52* (10), 3366–3376.

(41) Guile, S. D.; Alcaraz, L.; Birkinshaw, T. N.; Bowers, K. C.; Ebden, M. R.; Furber, M.; Stocks, M. J. Antagonists of the P2X₇ receptor. From lead identification to drug development. *J. Med. Chem.* **2009**, *52* (10), 3123–3141.

(42) Abberley, L.; Bebius, A.; Beswick, P. J.; Billinton, A.; Collis, K. L.; Dean, D. K.; Fonfria, E.; Gleave, R. J.; Medhurst, S. J.; Michel, A. D.; Moses, A. P.; Patel, S.; Roman, S. A.; Scoccitti, T.; Smith, B.; Steadman, J. G. A.; Walter, D. S. Identification of 2-oxo-*N*-(phenylmethyl)-4-imidazolidinecarboxamide antagonists of the P2X₇ receptor. *Bioorg. Med. Chem. Lett.* **2010**, *20* (22), 6370–6374.

(43) Lee, G. E.; Lee, W. G.; Lee, S. Y.; Lee, C. R.; Park, C. S.; Chang, S.; Park, S. G.; Song, M. R.; Kim, Y. C. Characterization of protoberberine analogs employed as novel human P2X₇ receptor antagonists. *Toxicol. Appl. Pharmacol.* **2011**, *252* (2), 192–200.

(44) Lee, G. E.; Lee, H. S.; Lee, S. D.; Kim, J. H.; Kim, W. K.; Kim, Y. C. Synthesis and structure–activity relationships of novel, substituted 5,6-dihydrodibenzo[*a,g*]quinolizinium P2X₇ antagonists. *Bioorg. Med. Chem. Lett.* **2009**, *19* (3), 954–958.

(45) Kahlenberg, J. M.; Lundberg, K. C.; Kertesy, S. B.; Qu, Y.; Dubyak, G. R. Potentiation of caspase-1 activation by the P2X₇ receptor is dependent on TLR signals and requires NF-kappa B-driven protein synthesis. *J. Immunol.* **2005**, *175* (11), 7611–7622.

(46) Lee, G. E.; Joshi, B. V.; Chen, W.; Jeong, L. S.; Moon, H. R.; Jacobson, K. A.; Kim, Y. C. Synthesis and structure–activity relationship studies of tyrosine-based antagonist at the human P2X₇ receptor. *Bioorg. Med. Chem. Lett.* **2008**, *18* (2), 571–575.

(47) Nakamura, T.; Kodama, N.; Arai, Y.; Kumamoto, T.; Higuchi, Y.; Chaichantipyuth, C.; Ishikawa, T.; Ueno, K.; Yano, S. Inhibitory effect of oxycoumarins isolated from the Thai medicinal plant *Clausena guillauminii* on the inflammation mediators, iNOS, TNF-α, and COX-2 expression in mouse macrophage RAW 264.7. *J. Nat. Med.* **2009**, *63* (1), 21–27.

(48) Gilroy, D. W.; Tomlinson, A.; Willoughby, D. A. Differential effects of inhibition of isoforms of cyclooxygenase (COX-1, COX-2) in chronic inflammation. *Inflammation Res.* **1998**, *47* (2), 79.

(49) Gendron, F.-P.; Hill, L. M.; Lenertz, L. Y.; Karta, M. R.; Berics, P. J. Activation of the transcription factor FosB/activating protein-1 (AP-1) is a prominent downstream signal of the extracellular nucleotide receptor P2X₇R in monocytic and osteoblastic cells. *J. Biol. Chem.* **2010**, *285* (44), 344–352.

(50) Gendron, F.-P.; Chalimoniuk, M.; Strosznajder, J.; Shen, S.; González, F. A.; Weisman, G. A.; Sun, G. Y. P2X₇ nucleotide receptor activation enhances IFNγ-induced type II nitric oxide synthase activity in BV-2 microglial cells. *J. Neurochem.* **2003**, *87* (2), 344–352.

(51) Goggins, M. G.; Shah, S. A.; Goh, J.; Cherukuri, A.; Weri, D. G.; Kellerher, D.; Mahmud, N. Increased urinary nitrite, a marker of nitric oxide, in active inflammatory bowel disease. *Mediators Inflammation* **2001**, *10* (2), 69–73.

(52) Van Dalen, C. J.; Winterbourn, C. C.; Senthilmohan, R.; Kettle, A. J. Nitrite as a substrate and inhibitor of myeloperoxidase. Implications for nitration and hypochlorous acid production at sites of inflammation. *J. Biol. Chem.* **2000**, *275* (16), 11638–11644.

(53) Davies, C. A.; Rocks, S. A.; O'Shaughnessy, M. C.; Perrett, D.; Winyard, P. G. Analysis of nitrite and nitrate in the study of inflammation. *Methods Mol. Biol.* **2003**, *225* (3), 305–320.